

Scientific Excellence • Resource Protection & Conservation • Benefits for Canadians  
Excellence scientifique • Protection et conservation des ressources • Bénéfices aux Canadiens

DFO - Library / MPO - Bibliothèque



10018564

## ANALYSIS OF SNOW THICKNESS DATA COLLECTED BY IMPULSE RADAR OVER THE BEAUFORT SEA SHELF IN 1991

L.A. Lalumiere

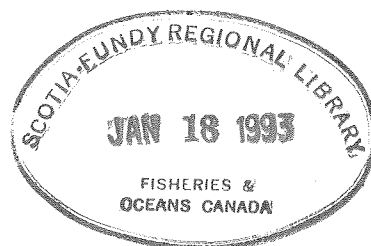
*Published by*

Physical and Chemical Sciences Branch  
Scotia-Fundy Region  
Department of Fisheries and Oceans

Bedford Institute of Oceanography  
P.O. Box 1006  
Dartmouth, Nova Scotia  
Canada B2Y 4A2

1992

Canadian Contractor Report of  
Hydrography and Ocean Sciences  
No. 43



Fisheries  
and Oceans

Pêches  
et Océans

Canada

## **Canadian Contractor Report of Hydrography and Ocean Sciences**

Contractor reports are unedited final reports from scientific and technical projects contracted by the Ocean Science and Surveys (OSS) sector of the Department of Fisheries and Oceans.

The contents of the reports are the responsibility of the contractor and do not necessarily reflect the official policies of the Department of Fisheries and Oceans.

If warranted, contractor reports may be rewritten for other publications of the Department, or for publication outside the government.

Contractor reports are abstracted in *Aquatic Sciences and Fisheries Abstracts* and indexed in the Department's annual index to scientific and technical publications.

Contractor reports are produced regionally but are numbered nationally. Requests for individual reports will be filled by the issuing establishment listed on the front cover and title page. Out of stock reports will be supplied for a fee by commercial agents.

Regional and headquarters establishments of Ocean Science and Surveys ceased publication of their various report series as of December 1981. A complete listing of these publications is published in the *Canadian Journal of Fisheries and Aquatic Sciences*, Volume 39: Index to Publications 1982. The current series, which begins with report number 1, was initiated in January 1982.

## **Rapport canadien des entrepreneurs sur l'hydrographie et les sciences océaniques**

Cette série se compose des rapports finals non révisés préparés dans le cadre des projets scientifiques et techniques réalisés par des entrepreneurs travaillant pour le service des Sciences et levés océaniques (SLO) du ministère des Pêches et des Océans.

Le contenu des rapports traduit les opinions de l'entrepreneur et ne reflète pas nécessairement la politique officielle du ministère des Pêches et des Océans.

Le cas échéant, certains rapports peuvent être rédigés à nouveau de façon à être publiés dans une autre série du Ministère, ou à l'extérieur du gouvernement.

Les rapports des entrepreneurs sont résumés dans la publication *Résumés des sciences halieutiques et aquatiques* et ils sont classés dans l'index annuel des publications scientifiques et techniques du Ministère.

Les rapports des entrepreneurs sont produits à l'échelon régional, mais numérotés à l'échelon national. Les demandes de rapports seront satisfaites par l'établissement auteur dont le nom figure sur la couverture et la page du titre. Les rapports épuisés seront fournis contre rétribution par des agents commerciaux.

Les établissements des Sciences et levés océaniques dans les régions et à l'administration centrale ont cessé de publier leurs diverses séries de rapports en décembre 1981. Une liste complète de ces publications figure dans le volume 39, Index des publications 1982 du *Journal canadien des sciences halieutiques et aquatiques*. La série actuelle a commencé avec la publication du rapport numéro 1 en janvier 1982.

Canadian Contractor Report of  
Hydrography and Ocean Sciences No. 43

1992

ANALYSIS OF SNOW THICKNESS DATA  
COLLECTED BY IMPULSE RADAR  
OVER THE BEAUFORT SEA SHELF IN 1991

by

Louis A. Lalumiere<sup>1</sup>

Physical and Chemical Sciences Branch  
Scotia-Fundy Region  
Department of Fisheries and Oceans

Bedford Institute of Oceanography  
P.O. Box 1006  
Dartmouth, Nova Scotia  
Canada, B2Y 4A2

---

<sup>1</sup>Canpolar Inc., 265 Rimrock Road, Unit 4, Downsview, Ont., Canada M3J 3C6

Prepared under DSS Contract No. FP 957-1-0834/01-OSC. Published by the Department of Fisheries and Oceans for the sea-ice program at the Bedford Institute of Oceanography through funds of the Federal Panel of Energy and Development.

© Minister of Supply and Services Canada, 1992  
Cat. No. FS 97-17/43E ISSN: 0711-6748

Correct citation for this publication:

Lalumiere, L.A. 1992. Analysis of Snow Thickness Data Collected by Impulse Radar over the Beaufort Sea Shelf in 1991. Can. Contr. Rep. of Hydrogr. and Ocean Sci. No 43: viii + 73 pp.

## Table of Contents

<b>Abstract</b>	Page iv
<b>Table Captions</b>	v
<b>Figure Captions</b>	vi
<b>1. Introduction</b>	1
<b>2. Equipment description</b>	1
2.1 Radar Hardware	1
2.2 Equipment Operation	2
2.3 Processing Tools	2
<b>3. Site Descriptions</b>	3
3.1 Shear Ridge Site	3
3.2 Ice Road Site	4
3.3 IOS Ridge Site and Calibration Lead Site	4
3.4 ESSO Site	4
3.5 GPS Track Plots	5
<b>4. Discussion</b>	5
4.1 Processing Radar Data for Snow Thickness	5
4.1.1 Pre-processing of the Radar Data	5
4.1.2 Snow Thickness Inversion Algorithm	7
4.1.3 Snow Thickness Results	9
4.2 Combined EM/Radar System	9
4.3 Automatic Levelling of Ice Surface in Hard-copy Plots	10
<b>5. Conclusions and Recommendations</b>	11
<b>Acknowledgement</b>	12
<b>References</b>	13
<b>Tables</b>	13
<b>Figures</b>	18
<b>Appendix A:</b> Listing of processing routines	
<b>Appendix B:</b> Histograms of snow thickness at marker positions for lines SHEAR2 and SHEAR3	

## ABSTRACT

Lalumiere, L.A. 1992. Analysis of Snow Thickness Data Collected by Impulse Radar over the Beaufort Sea Shelf in 1991. Can. Contr. Rep. of Hydrogr. and Ocean Sci. No 43: viii + 73 pp.

A helicopter-borne ground penetrating radar sensor profiled over five sites during Arctic field trails near Tuktoyaktuk, NWT, during April 1991. The sites were the shear ridge site, IOS ridge site, the calibration lead, the ice road and the ESSO site, with several profiles over each site.

Radar data plotting and processing tools were developed to enable presentation of the data in a form useful for the further development of an algorithm to process radar data for snow thickness.

The refinement of previous work on the snow thickness algorithm included the development of some pre-processing steps to condition the radar data, the measurement of noise levels to determine the operational height range of the sensor and the addition of flags indicating where no snow thickness measurement is possible due to surface or operational conditions.

Comparisons were made of the results from the snow thickness inversion algorithm versus surface information for two passes over the shear ridge site. The algorithm appears to work well for Arctic conditions when the snow is more than 20 cm thick.

Using results from the snow thickness processing, an automated alignment routine was developed to remove helicopter height variation effects, to make hard copy-copy plots of radar data easier to interpret.

## Résumé

Lalumiere, L.A. 1992. Analysis of Snow Thickness Data Collected by Impulse Radar over the Beaufort Sea Shelf in 1991. Can. Contr. Rep. of Hydrogr. and Ocean Sci. No 43: viii + 73 pp.

Un capteur de géoradar héradar héliporté a relevé, pendant des essais sur le terrain dans l'Arctique, près de Tuktoyaktuk (TNO) en avril 1991, plusieurs profils de chacun des cinq emplacements suivants: la crête de cisaillement, la crête de l'ISM, la fissure d'étalonnage, la route de glace et l'installation d'ESSO.

Des outils de traçage et de traitement des données radar ont été mis au point pour permettre de présenter les données sous une forme utile en vue du perfectionnement d'un algorithme automatisé de traitement des données radar sur l'épaisseur de neige.

Les derniers travaux d'amélioration de l'algorithme comprenaient des étapes de prétraitement pour conditionner les données radar, des mesures de bruit pour déterminer la plage d'altitude de fonctionnement du capteur et l'addition de fanions indiquant les endroits où il est impossible de mesurer l'épaisseur de neige à cause des conditions de surface ou de fonctionnement. Les résultats de l'algorithme d'inversion de l'épaisseur de neige ont été comparés aux données de surface pour deux passages audessus de la crête de cisaillement. L'algorithme semble bien fonctionner dans l'Arctique lorsqu'il y a plus de 20 cm de neige.

Les résultats du traitement des données sur l'épaisseur de neige ont permis d'élaborer un programme de lissage automatisé qui élimine les effets des variations d'altitude de l'hélicoptère, ce qui permit des tracés sur papier des données radar plus faciles à interpréter.

### Table Captions

- Table 1. A comparison of the results from the snow thickness inversion algorithm with surface observations for radar profiles collected at the shear ridge site on April 16, 1991.
- Table 2. Surface conditions for ice road radar profile collected April 9, 1991. Flown from south to north.
- Table 3. Surface conditions for ice road radar profile collected April 16, 1991. Flown from north to south.
- Table 4. Surface conditions for radar profile collected at the ESSO site on April 16, 1991.

### Figure Captions

- Fig. 1      Snow thickness radar sensor block diagram.
- Fig. 2      Map showing locations of sites where radar profiles were made near Tuktoyaktuk NWT, during April 1991: station 1 - ice road; station 2 - ESSO site; station 3 shear ridge; station 4 - calibration site; station 5 - IOS ridge site. (from Prinsenberg et al.)
- Fig. 3      Sketch of shear ridge site, with the line direction shown with the arrow.
- Fig. 4 a)   Grey-scale plot of raw radar data from profile SHEAR2 over the shear ridge site, north section, flown April 16, 1991. The vertical axis is two-way travel time of the radar signal in nanoseconds. The horizontal axis is shown with trace numbers and metre position along the line. The height of surface features can be determined using 6.67 ns/m height. Snow thickness can be determined using 13.3 ns/m thickness. For example, the ridge at position 0 was 3 m high and the snow drift at trace number 800 was 0.5 m thick.
- Fig. 4 b)   Same as Fig. 4 a) but for the south section of the line.
- Fig. 5 a)   Grey-scale plot of raw radar data from profile SHEAR3, over shear ridge site, north section, flown April 16, 1991. The vertical axis is two-way travel time of the radar signal. The horizontal axis is shown with trace numbers and metre position along the line. The height of surface features can be determined using 6.67 ns/m height. Snow thickness can be determined using 13.3 ns/m thickness.
- Fig. 5 b)   Same as Fig. 5 a) but for the south section of the line.
- Fig. 6      Grey-scale plot of raw radar data from a profile over the ice road site, flown April 9, 1991. Table 1 lists surface conditions versus trace numbers along the profile. The vertical axis is two-way travel time of the radar signal in nanoseconds. The horizontal axis is trace (scan) number as collected along the profile. Note the echo from the ice/water interface.
- Fig. 7      Grey-scale plot of raw radar data from a profile over the ice road site, flown April 16, 1991. Table 2 lists surface conditions versus trace numbers along the profile. The vertical axis is two-way travel time of the radar signal in nanoseconds. The horizontal axis is trace (scan) number as collected along the profile. Note the echo from the ice/water interface.



- Fig. 8 Grey-scale plot of raw radar data from the profile over the IOS ridge site, flown April 19, 1991. The vertical axis is in number of bins (samples). Each bin represents 0.22 ns in two-way travel time. There is no ground referencing as there was no video imagery for this profile.
- Fig. 9 Grey-scale plot of raw radar data from the profile over the ESSO site, flown April 16, 1991. Table 3 lists surface conditions versus trace numbers along the profile. The vertical axis is two-way travel time of the radar signal in nanoseconds. The horizontal axis is trace (scan) number as collected along the profile.
- Fig. 10 GPS track plot for 2 profiles over the ice road site, flown April 16, 1991. The vertical axis is decimal degrees north latitude offset from  $69^{\circ}$  N latitude. The horizontal axis is decimal degrees west longitude offset from  $133^{\circ}$  W longitude. The track marked AL2 corresponds to the profile plotted in Fig. 7.
- Fig. 11 GPS track plot for the profiles over the ESSO site, flown April 16, 1991. The vertical axis is decimal degrees north latitude offset from  $69^{\circ}$  N latitude. The horizontal axis is decimal degrees west longitude offset from  $133^{\circ}$  W longitude. The GPS track corresponds to the profile plotted in Fig. 9.
- Fig. 12 GPS track plot for the 3 profiles at the shear ridge site, flown April 16, 1991. The vertical axis is decimal degrees north latitude offset from  $69^{\circ}$  N latitude. The horizontal axis is decimal degrees west longitude offset from  $133^{\circ}$  W longitude. The radar data for the track marked SHEAR2 is plotted in Fig. 4. The radar data for the track marked SHEAR3 is plotted in Fig. 5.
- Fig. 13 Oscilloscope plot of the last 512 samples of the first trace from profile SHEAR3.  
 a) raw unprocessed data.  
 b) band-pass filtered from 250 MHz to 1250 MHz.  
 c) band-pass filtered from 125 MHz to 612.5 MHz.
- Fig. 14 Results of background subtraction processing on the entire 1024 samples of trace 1 of profile SHEAR3.  
 a) band-passed filtered data (125 MHz to 612.5 MHz).  
 b) Resulting trace after background subtraction.  
 c) RMS voltage levels for traces shown in Fig. 14 a) and 14 b).
- Fig. 15 Variable area plot of radar data from profile SHEAR3, traces 736 to 790. The first echo seen in each trace is from the top of a snow drift. The second echo is a reflection from the snow/ice interface.

- Fig. 16 a) Snow thickness surface measurements taken at the shear ridge site. Measurements were taken at 5 m intervals using a hand probe on April 17, 1991.
- Fig. 16 b) Automated results for the snow thickness radar for profile SHEAR2 at the shear ridge site, flown April 16, 1991.
- Fig. 16 c) Automated results for the snow thickness radar for profile SHEAR3 at the shear ridge site, flown April 16, 1991.
- Fig. 17 Noise analysis of radar data when system flown with the EM sensor. Oscilloscope plots individual radar traces.
- a) Radar only.
  - b) EM console turned on, EM transmitters in bird turned off.
  - c) as b) with EM transmitters in bird turned on.
- Fig. 18 Power spectral density plots of each trace shown in Fig. 17.
- Fig. 19 a) Grey-scale plot of aligned radar data profile SHEAR2 over shear ridge site, north section. Using results from the snow thickness processing, helicopter height variations have been removed. The vertical axis is two-way travel time in ns, but after alignment processing, only relative time measurements can be made. A plot of the un-aligned data is shown in Fig 4.
- Fig. 19 b) Same as Fig. 19 a) but for the south section of the line.
- Fig. 20 Grey-scale plot of aligned radar data profile SHEAR3 over shear ridge site, north section. Using results from the snow thickness processing, helicopter height variations have been removed. The vertical axis is two-way travel time in ns, but after alignment processing, only relative time measurements can be made. A plot of the un-aligned data is shown in Fig 5.
- Fig. 20 b) Same as Fig. 20 a) but for the south section of the line.

## 1. Introduction

During April 1991, field trials of a newly developed helicopter-mounted snow and ice thickness sensor were performed near Tuktoyaktuk, NWT. The snow and ice thickness sensor included an EM induction instrument, a laser profilometer and a recently added component, ground penetrating radar. The ground penetrating radar (GPR) was flown by itself and as part of the combined sensor. The field work and initial development of the software routines to process the radar data were funded by previous contracts. This report documents work performed to further analyze the radar data collected during the Tuk '91 field program and to develop a robust snow thickness inversion algorithm for the future development of a real-time snow thickness sensor.

## 2. Equipment Description

### 2.1 Radar Hardware

The impulse radar system contained a GSSI SIR 7 control unit, a GSSI 3102DP transducer, a tow cable, an analog tape recorder and a lap-top computer for digital data acquisition. Fig. 1 is a sketch of the snow radar equipment.

The control unit was used to set the position and length of the radar range window and to distribute power and timing signals to the transducer via the tow cable. A Panasonic AG-7400 S-VHS VCR recorded the audio frequency signals from the radar transducer during the entire time the helicopter was airborne. Digital recordings were made with a Toshiba T3100SX lap-top with a Data Translation DT-2812 A/D board. The cable connecting the control unit in the helicopter and the transducer in the bird had an emergency release quick-disconnect connection.

The GSSI model 3102DP transducer operated with a 500 MHz centre frequency and had a pulse length of 3 ns. The radar control unit was set to replicate the radar signal at 12.8 scans per second with a window length of 255 ns. The A/D board sampling frequency was 15,000 Hz and 1024 samples were collected over each scan. With an effective radio frequency sampling interval of 220 ps and the time zero position at sample number 72, the remaining window length was 223 ns. A more detailed description of the radar hardware can be found in the TDC report TP11282E (Holladay et al.) Fig 4. is an example plot of a profile of radar data.

## 2.2 Equipment Operation.

With an effective radar range window of about 220 ns the maximum flying height for the radar antenna over the ice surface was 33 m. In the plot of radar data shown in Fig. 3, the dark bands running the length of the profile in the first 100 ns of the radar range window limits the minimum height to 15 m. With a scan rate of 12.8 scans per second and a helicopter ground speed of approximately 25 km/hr a radar scan was collected every half metre along the profile lines.

Digital data acquisition began when the helicopter was on line and helicopter altitude was below 33 m. Markers were placed in the digital data set when the antenna was observed to be over ground control points.

## 2.3 Processing Tools

The radar data set collected at Tuktoyatuk caused problems for the usual computer tools available for radar data processing. Radar profiles with 1024 points per scan were double the usual length and long profiles of about 2000 scans made file sizes of about four megabytes. Plotting routines and processing techniques were developed to handle the large data files.

Variable area plots (like the one shown in Fig. 16) were good for showing detailed amplitude and phase changes but produce plots of awkward length. Also, since the available variable area plotting routines could not print the large number of points in each scan as one profile, the plots had to be broken into top and bottom parts.

A high resolution grey-scale plotting routine was developed which could handle the large data volumes and print the data at a much higher density than the variable area plots. The grey-scale plotting routine produces output for a POSTSCRIPT printer. Each pixel can be printed at 16 or 256 shades of grey and the physical size of the pixel can be chosen for full control of the aspect ratio of the radar plot. The plotting program accepts data in 16 bit binary format or in MATLAB data file format. The plotting program was designed to run in batch mode due to the long time required to print a profile of radar data. All the grey-scale radar plots in the report were produced using this new program.

Prior to plotting and processing for snow thickness the radar data were filtered using a digital zero-phase filter. A second order Butterworth IIR filter with a pass

band of 250 MHz to 1.25 GHz was applied in both directions to each radar trace. This applies a fourth order filter with no phase change.

### 3. Site Descriptions

A helicopter-borne ground penetrating radar (GPR) profiled over five sites during Arctic field trials near Tuktoyaktuk, NWT, during April 1991 (Prinsenberg et al.). The sites were the shear ridge site, IOS ridge site, the calibration lead, the ice road site and the ESSO site, with several profiles over each site (Fig. 2). Ancillary data were collected of auger ice and snow thickness; snow, ice and water salinities.

Of the five sites, only data from the shear ridge site was useful in the development and testing of the automated snow thickness inversion algorithm.

#### 3.1 Shear Ridge Site

Three profiles were made over the shear ridge site on April 16, 1991. The first profile attempt has not been analyzed as the helicopter flew far off the marked line and the battery powering the video recorder died just after the ridge was passed. The second profile (data file called SHEAR2) over the line produced good data but the video recorder was off for most of the line, so that recording took place only over the last three bags. The third profile (SHEAR3) had complete video coverage and from the video tape record, the radar antenna can be seen to follow about five to ten metres to the right (west side) of the marked line.

Fig. 3 is a sketch of surface features of a north-south transect approximately 1 km long over the shear ridge site. Zero position on the line was centred over the shear ridge. The area from -100 m to 0 m in line coordinates was flat with very thin snow cover. From -100 m to -200 m the surface condition was that of a rough (ice pieces of 0.5 m to 1.5 m) rubble field. From -200 m to -400 m the surface alternated between small, smooth areas (10 m - 20 m diameter) and rough, broken-up areas (about 1 m size pieces). To the south of the ridge, from 0 m to 150 m, there were three large drifts of snow. The transect crossed a small ridge, centred at 200 m. From 220 m to 500 m, the ice was flat with snow cover varying from 0 m to 0.3 m in small drifts. The hard-copy plots of filtered radar data from lines SHEAR2 and SHEAR3 and shown respectively in Fig. 4 and 5. Table 1 compares the surface information with the two radar profiles over the shear ridge site.

### 3.2 Ice Road Site

The ice road site was accessible by truck and was visited several times for the collection of surface information and making surface profiles with the radar. Also as the ice road site was close to the Polar Continental Shelf Project facility, we were able to fly helicopter-borne profiles over it several times on different days. While useful for checking the radar equipment and comparing ground radar data with airborne radar data, the ice road site was not useful in the development of the automated snow thickness algorithm. Also, the nearby DEW station's radar interfered with the snow thickness radar each time it swept through the direction of the ice road site. Fig. 6 is a plot of the radar data over the ice road site flying from south to north on April 9, 1991. Table 2 lists the surface information at the ice road site versus trace numbers for radar profile from April 9. Fig. 7 is a plot of the radar data over the ice road site flying from north to south on April 16, 1991. Table 3 lists the surface information at the ice road site versus trace numbers for the radar profile from April 16.

### 3.3 IOS Ridge Site and Calibration Lead Site

The IOS ridge site and the calibration lead site were only profiled with the radar in the bird with the EM system. Due to the high noise levels from the EM system, this data was not processed for snow thickness. Fig. 8 is a plot of the radar data over the IOS ridge site collected on April 19, 1991, after band-pass filtering each trace in the plot.

### 3.4 ESSO Site

The ESSO site was visited on April 16, 1991. It was a grounded man-made ice platform of spray ice and contained NRC's ice motion and ice stress instruments (Prinsenberg et al.). To the side of the grounded ice mound was an area about 30 m by 100 m with snow about 50 to 100 cm thick. Surface snow thickness measurements were taken in a grid fashion over the snow area with the hope of seeing in the video the part of the grid profiled with the radar. On viewing the video tape later, it was not possible to determine the section of the gridded area flown over. Fig. 9 is a plot of the radar data over the ESSO site, flown on April 16, 1991. Table 4 lists the surface information at the ESSO site versus the trace numbers for the radar profile.

### 3.5 GPS Track Plots

On April 16, 1991, a GPS positioning system was used to track the helicopter's position as it profiled over the ice road site (Fig. 10), the ESSO site (Fig. 11) and the Shear Ridge site (Fig. 12). GPS positions were not taken for the bags marking the lines, and as a result it was not possible to draw the true surface position of the lines on the GPS track plots. In the GPS track plot for the shear ridge site (Fig. 12), line SHEAR1 can be seen wandering off line a few times. Line SHEAR2 and SHEAR3 follow very closely over the same track. The shear ridge was located at  $69^{\circ} 53' 25''$  N latitude,  $133^{\circ} 01' 04.4''$  W longitude put making the GPS tracks in Fig. 12 out by about 200 m. The other GPS track plots were also offset by 200 m to the west.

## **4. Discussion**

### 4.1 Processing Radar Data for Snow Thickness

The snow thickness inversion algorithm has been refined and several features have been added to make it more robust than the version described in the TDC report (Holladay et al.). Analysis has been made on some of the parameters that were used in the algorithm and the steps needed for snow thickness processing are outlined.

Two lines from the shear ridge site were used to refine the snow thickness inversion algorithm. The lines were SHEAR2 and SHEAR3 and are described above in the site description section.

#### 4.1.1 Pre-processing of the Radar Data.

Before processing the radar data for snow thickness, some pre-processing was performed on the data to remove as much noise as possible and to provide information for the snow thickness inversion algorithm.

#### **Filtering**

Each trace was band-pass filtered to remove high frequency random noise and low frequency noise. The filter weights were chosen to adjust the pulse shape to keep side lobes at a minimum. The pulse shape has a large central impulse with smaller peaks on either side. Normally, the radar data was band-pass filtered

around the bandwidth of the antenna elements, in this case the upper cut-off frequency was decrease side lobe ringing. This step also increased the pulse length somewhat, reducing resolution. Fig. 13 compares different filtering applied to trace number 521 from radar line SHEAR3 over an area of bare ice. Fig. 13 a) is a plot of the trace without filtering (only the last 512 points were plotted). Fig. 13 b) is a plot of the trace band-pass filtered from 250 MHz to 1.25 GHz. Fig. 13 c) is a plot of the trace band-pass filtered from 125 MHz to 620 MHz. Fig. 13 a) and b) compare very similarly except for the removal of the DC component and high frequency noise. The small side lobe before the large peak was 6 dB over the background RMS noise level and the large peak was 26 dB over background noise level. In Fig. 13 c) the small side lobe before the large peak was down to the level of the background noise and the large peak has been reduced to 22.5 dB. The pulse length has been increased by about fifty percent, increasing the minimum resolvable snow thickness from 15 cm to 25 cm.

#### Background Subtraction

The first 100 ns of the radar range window contains large ringing signals. These are seen as dark bands running along the top of a profile as seen in Fig. 4. The ringing noise was caused by the close proximity of the pulser to the receiver. The ringing was the same for each radar trace and a large portion of it can be removed from the data by background subtraction. Lines SHEAR2 and SHEAR3 have sections where the ice surface was beyond the end of the radar range window. These sections were extracted, stacked (averaged) into one trace and then filtered using the same filter weights as the rest of the radar profile.

The reduction in the ringing by background subtraction allows snow thickness measurements to be made at lower flying altitudes. The minimum flying altitude without background subtraction was 15 m. With background subtraction minimum flying altitude was reduced to 9 m. Fig. 14 a) is trace 1 from line SHEAR3 before background subtraction. Fig. 14 b) is the same trace after background subtraction. A plot of the RMS voltage levels over a 30 bin window for each trace is shown in Fig. 14 c).

A problem in the rf connections in the tow cable caused the ringing to change during some of the early flights made during the Tuk '91 field program (Fig. 6 - Ice road site on April 9, 1991). The new hardware configuration built for the St. Anthony '92 field put all rf components of the radar in the bird, removing this problem.



## RMS Noise Levels

After filtering and background subtraction, a running measure of the RMS noise level was made down the length of a trace. The window size for the RMS measurements was 10 bins, roughly the number of samples in the period of a signal at 500 MHz. Typically only one RMS noise measurement needs to be made for a given radar profile.

## Peak Transform

The previous processing steps condition the data in preparation for extracting all of all the peaks in the data set. Each trace has a smoothing difference function applied to it to convert all peak locations to zero crossings. The difference function works by taking the difference of a sliding average on both sides of every point in a radar trace. The sensitivity to peak size was controlled by the number of points used to make the average. Currently, two points on each side of the current point were used to make the average. The position of the zero crossings were easily located and peak values from the pre-processed data set were stored in the location of the zero crossings.

### 4.1.2 Snow Thickness Inversion Algorithm

To process the radar data for snow thickness, a model was established as a basis for classifying peaks as ice echoes or snow echoes.

The model uses the following assumptions:

- radar footprint diameter was approximately equal to antenna height
- over a smooth flat reflector most of the energy was returned from a region with a radius less than one tenth antenna height (first Fresnel zone)
- small radar targets (in a rubble field) return echoes with much smaller amplitudes than large flat targets (flat ice)
- the echo from the ice surface (whether covered by snow or not) has the largest amplitude in the trace
- the echo from the air/snow interface was the largest signal (over random noise levels) that arrives before the ice echo.

No snow thickness determination was made if:

- 1 - the ice echo was smaller than the snow echo threshold
- 2 - the ice/snow surface was beyond the end of the radar range window.

For every trace in a radar profile, the maximum peak value was found and its value and location were stored. This peak might correspond to an echo from the top of the ice.

The data were then searched for the first peak after a chosen start position, that was over a given threshold. For every trace in a radar profile the peak value and location of the first echo over the threshold was stored as a possible snow surface echo. If there was no snow then this echo will be from the top of the ice. The start position and threshold were chosen by comparing the typical amplitude of the echo from the air/snow interface and the background RMS noise levels. A variable area plot of traces 736 to 790 (Fig. 15) in line SHEAR3 shows echoes from the air/snow interface and the snow/ice interface. The mean value for the amplitude of the snow echo was 165 bit levels with a standard deviation of 30 bit levels. In the lower 512 samples, the RMS noise level varies down the length of a pre-processed trace from 5 bit levels to 1 bit level (Fig. a)). A value of 50 bit levels was chosen as the threshold value as it allowed detection of all of the snow echoes seen on the hard-copy plots of lines SHEAR2 and SHEAR3.

A few logical conditions were performed on the position and value of the ice and snow echoes to flag when certain conditions occur. If no peak was over the threshold and the ice peak was smaller than the threshold then the snow thickness was set to zero and a flag was set indicating that no peak was found so the surface was beyond the end of the radar range window. If the ice peak value was greater than the RMS noise level but less than the threshold then the snow thickness was set to zero and a flag was set indicating that the ice peak was too small, probably due to a rough surface scattering the radar echo.

As no trace-to-trace tracking of the snow or ice echoes was performed, some smoothing was required to reduce the effect of incorrect positioning of the ice or snow echoes, using a second-order Butterworth IIR low-pass filter along track. The ice echo position was filtered with a normalized cut-off frequency of  $0.05 \text{ m}^{-1}$ , representing a surface footprint size of about 20 m. The snow echo position was filtered with a normalized cut-off frequency of  $0.2 \text{ m}^{-1}$ , representing a surface footprint size of 5 m. The cut-off frequency of  $0.5 \text{ m}^{-1}$  for low pass filtering the ice echo position was chosen as it provided adequate smoothing without removing the general surface variations due to helicopter height changes. The snow echo

positions were smoothed over a smaller footprint as the snow thickness changes at a greater rate than helicopter height variations.

To calculate snow thickness from the position of the ice and snow echoes, the radar velocity in the snow must be known. During the Tuktoyaktuk field program, detailed ground radar profiles over snow drifts of measured thickness gave a velocity 0.15 m/ns. Converting the sample position of the ice and snow echo to time in nanoseconds was performed using the sampling interval of 0.22 ns. The difference in time between the ice echo and the snow echo represents the two-way travel time of the radar signal in the snow layer. Dividing the two-way travel time in half, then multiplying by the radar velocity in the snow gives snow thickness.

Appendix A contains listing of the processing routines used to process the radar data for snow thickness.

#### 4.1.3 Snow Thickness Results

Lines SHEAR2 and SHEAR3 were processed for snow thickness using the above algorithm. The snow thickness results are similar, but as the radar sensor did not fly exactly along the same line, the snow drift cross-sections are different. Fig. 16 a) is a plot of the surface measurements for snow thickness taken on April 17, 1991. Fig. 16 b) is a plot of the results of snow thickness processing for the line SHEAR2. Fig. 16 c) is a plot of the results of snow thickness processing for the line SHEAR3.

Table 1 compares the snow thickness results from lines SHEAR2 and SHEAR3 with surface measurements and observations.

Appendix B contains histograms of snow thickness at each bag on lines SHEAR2 and SHEAR3. The histograms were taken from an area 10 metres on either side of each bag.

#### 4.2 Combined EM/Radar System

When the radar was flown in the bird with the EM system, large interference in the radar data was observed. Fig. 8 is a plot of the radar data digitized from tape of a profile over the IOS ridge site.

Noise from the EM system was large enough to mask the radar echoes from the surface. The noise was correlated with the radar data as the radar's receiver samples the RF signals at the antenna at 51.2 kHz. The high frequency used in the EM system was about 100 kHz which produced an aliased frequency in the data. The low frequency EM channel (about 2 kHz) also introduced noise. Fig. 17 a) is a plot of radar data when flown alone without the EM system. Fig. 17 b) is a plot of the radar data digitized from tape after the flight with the EM transmitters turned off. Fig. 17 c) is a plot of the radar data digitized from tape after the flight with the EM transmitters turned on. Fig. 18 is a plot of the power spectral density of each trace in Fig. 17. The radar trace digitized from tape data has higher noise levels than the radar trace digitized during the flight. Centred at 900 Hz was a noise spike common only to the radar data digitized from tape. Two large spikes at 1600 Hz and 2500 Hz were seen in the plot with the EM transmitters turned on.

Hardware changes to the snow thickness radar sensor for the March 1992 field trip to St. Anthony have reduced the noise from the EM system to a low enough level to remove the need to develop special filters to fix the problem. Also, special attention to the recording levels on the VCR ensured that tape noise levels were lower by a few dB than radar noise levels.

#### 4.3 Automatic Levelling of the Ice Surface in Hard-copy Plots

An automatic alignment technique was developed using data generated from the snow thickness inversion algorithm. The position of the ice echo was used for the most part, but when the surface echo was beyond the end of the radar range window, the snow position was used instead. This reduces some of the large spikes in the ice echo position. The resulting data were low pass filtered with a normalized 3 dB cut off frequency of  $0.03 \text{ m}^{-1}$ , representing 33 m on the surface. Lines SHEAR2 and SHEAR3 covered the 800 m line with about 1600 radar traces. This represents ground coverage of two traces per metre. The smoothed results were fed into an alignment algorithm which moved each radar trace up or down so that the ice echo would be flat across the middle of the radar range window. Fig. 19 is a hard-copy plot of the line SHEAR2 after alignment. Fig. 20 is a hard-copy plot of the line SHEAR3 after alignment. A comparison of the radar data before and after alignment shows how the snow drifts are clearly seen in the aligned data in areas where the helicopter altitude change had a steep slope. Printouts of the routines used for the altitude alignment are included in Appendix A.

## 5. Conclusions and Recommendations

The snow thickness inversion algorithm works well over smooth surface conditions. Snow thickness estimates were made when the snow was greater than 25 cm thick. When the snow thickness was less than 25 cm, the snow thickness estimate was zero.

Rough surface conditions such as rubble fields, produce highly varied snow thickness results. Measured snow drifts within the rubble field and snow thickness estimates from the snow thickness algorithm were similar, but as the survey flights were not directly over the surface sampling points, the true performance of the algorithm cannot be judged. The results from the snow thickness algorithm in rough areas were probably a better indication of the height of the ice blocks over the mean ice surface level than the thickness of snow drifts amongst the rubble.

Further testing of the snow thickness inversion algorithm is required before an accurate determination can be made on the algorithm's performance. Radar data from different snow and ice conditions should be processed using to determine how well the model on which the algorithm was based, holds up.

### Acknowledgements

We gratefully acknowledge Dr. Simon Prinsenberg of the Bedford Institute of Oceanography for his support for the further development of the snow thickness sensor as well as his assistance during data and ground truth collection in the field. Dr. Scott Holladay of Aerodat Limited is thanked for his encouragement of this work from the first thoughts of adding snow thickness radar to the EM ice thickness sensor in 1990. The staff of Aerodat were very helpful in the preparation for and during the Arctic field trial. Acknowledgement goes to the Polar Continental Shelf Project for provision of helicopter time, lodging and other logistic support at Tuktoyaktuk.

## References

Holladay, J.S., I.R. St. John, V. Schoegg, J. Lee, J.R. Rossiter and L.A. Lalumiere, 1992. Airborne EM ice Measurement Sensor - Phases 1-2. *Report to Transport Development Centre, Policy and Coordination, Transport Canada*. TP11282E: 67 pp.

Prinsenber, S.J., J.S. Holladay, J.R. Rossiter and L.A. Lalumiere, 1992. 1991 Beaufort Sea EM/Radar Ice and Snow Sounding Project. *Canadian Technical Report of Hydrography and Ocean Sciences*. No. 139: vi + 61 pp.

**Table 1.** A comparison of the results from the snow thickness inversion algorithm with surface observations for radar profiles collected at the shear ridge site on April 16, 1991.

Surface observations at Shear ridge site		Processing results from SHEAR2		Processing results from SHEAR3	
Bag #	Description from N to S	Trace #	Description	Trace #	Description
-300	Rough rubble field (pieces 50 to 100 cm in size). Drift of snow between ice pieces. Some areas of flat ice 20 m in diameter.	136	Surface beyond end of radar range window at bag.	112	At bag snow less than 20 cm. North of bag are three distinct drifts 30 to 45 cm in height.
-200	rubble field (pieces 1 m in size)	353	Snow drift up to 40 cm then Very rough results south of bag.	274	Surface beyond end of radar range window at bag location. very rough results to the south
-100	edge of rubble field. Smooth ice with very thin snow all the way to bag 0.	544	Solid return from ice surface. No snow.	455	Solid return from ice surface. No snow.



0	Top of shear ridge. To the south of the ridge there are three large snow drifts	721	Highly varied results at ridge. Large drift 50 m south of ridge closely matches surface info.	670	Large drift directly south of ridge. Shape of drift 50 m south of ridge closely resembles shape of drift defined by surface measurements.
100	Small ridge 10 m to the west. Small drifts 10 to 30 cm high.	905	Small drifts up to 20 cm. Large drift 40 to 60 cm high to south of small ridge.	850	Snow thickness 20 cm at bag. Large drift 80 to 100 cm high to the south of small ridge.
200	Drift 30 to 60 cm high	1098	20 to 30 of snow.	1050	20 to 30 cm of snow.
300	Snow from 0 to 20 cm depth	1353	0 to 20 cm at bag.	1289	Snow 0 to 20 cm at bag.
400	Snow from 0 to 20 cm depth	1538	0 to 20 cm of snow	1533	Snow 0 to 20 cm at bag.
500	Snow from 0 to 15 cm depth	1769	0 to 20 cm of snow	1788	Snow 0 to 20 cm at bag.

**Table 2. Surface conditions for ice road radar profile collected April 9, 1991. Flown from south to north.**

Trace number	Surface description
0-100	Snow banks from old ice road
100-215	Approx. 20 cm snow cover
215-225	South snow bank of ice road (90 cm high)
225-255	Ice road
255-270	Current north snow bank of ice road (160 cm high)
270-290	Old north snow bank (85 cm high)
290-315	Oldest north snow bank (95 cm high)
315-400	approx. 20 cm snow cover

**Table 3. Surface conditions for ice road radar profile collected April 16, 1991. Flown from north to south.**

Trace number	Surface description
1-280	0 to 20 cm snow cover
280-315	Oldest north snow bank of ice road (95 cm high)
330-360	Old north snow bank of ice road (85 cm high)
370-410	Current north snow bank of ice road (160 cm high)
410-460	Ice road
460-520	South snow bank (90 cm high)
520-800	Thin snow cover
800-930	Snow banks from old ice road

**Table 4.** Surface conditions for radar profile collected at the ESSO site on April 16, 1991.

Trace number	Surface description
0-200	Over artificial ice island
200-400	Snow thickness 50 - 80 cm
400-650	Ploughed ice road
650-700	Snow bank?
700-end	Surface out of radar range window

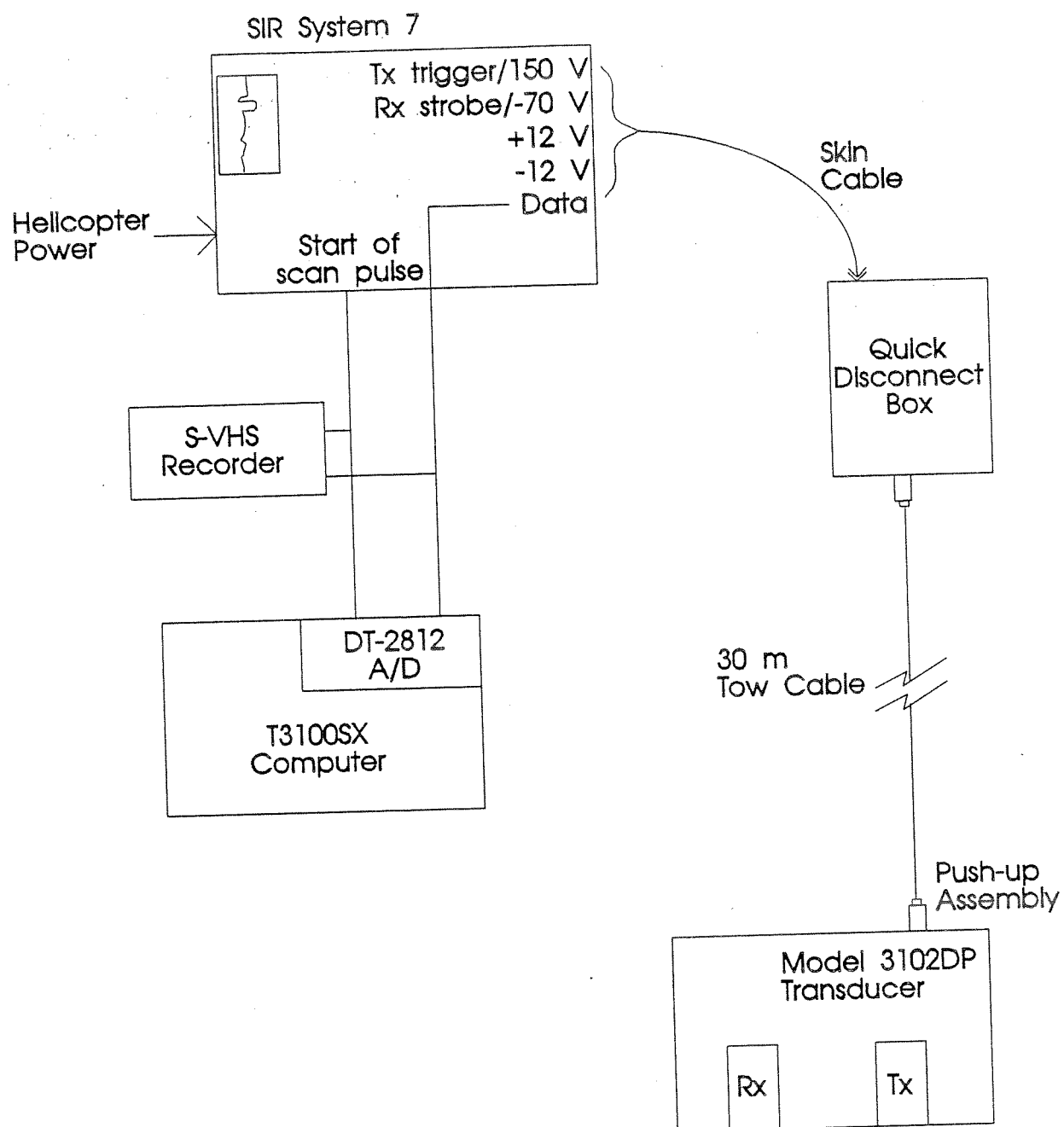


Fig. 1 - Snow thickness radar sensor block diagram.

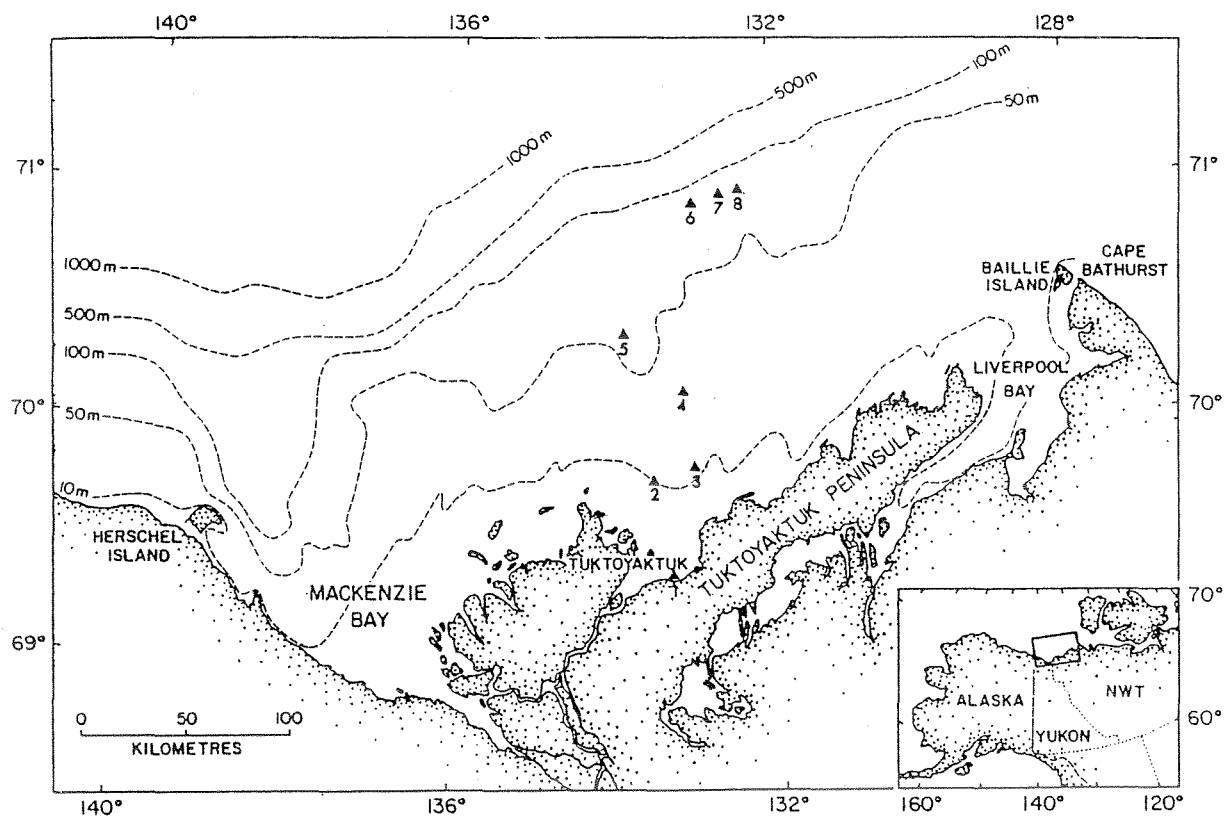


Fig. 2 Map showing locations of sites where radar profiles were made near Tukttoyaktuk NWT, during April 1991: station 1 - ice road; station 2 - ESSO site; station 3 shear ridge; station 4 - calibration site; station 5 - IOS ridge site. (from Prinsenberg et al.)

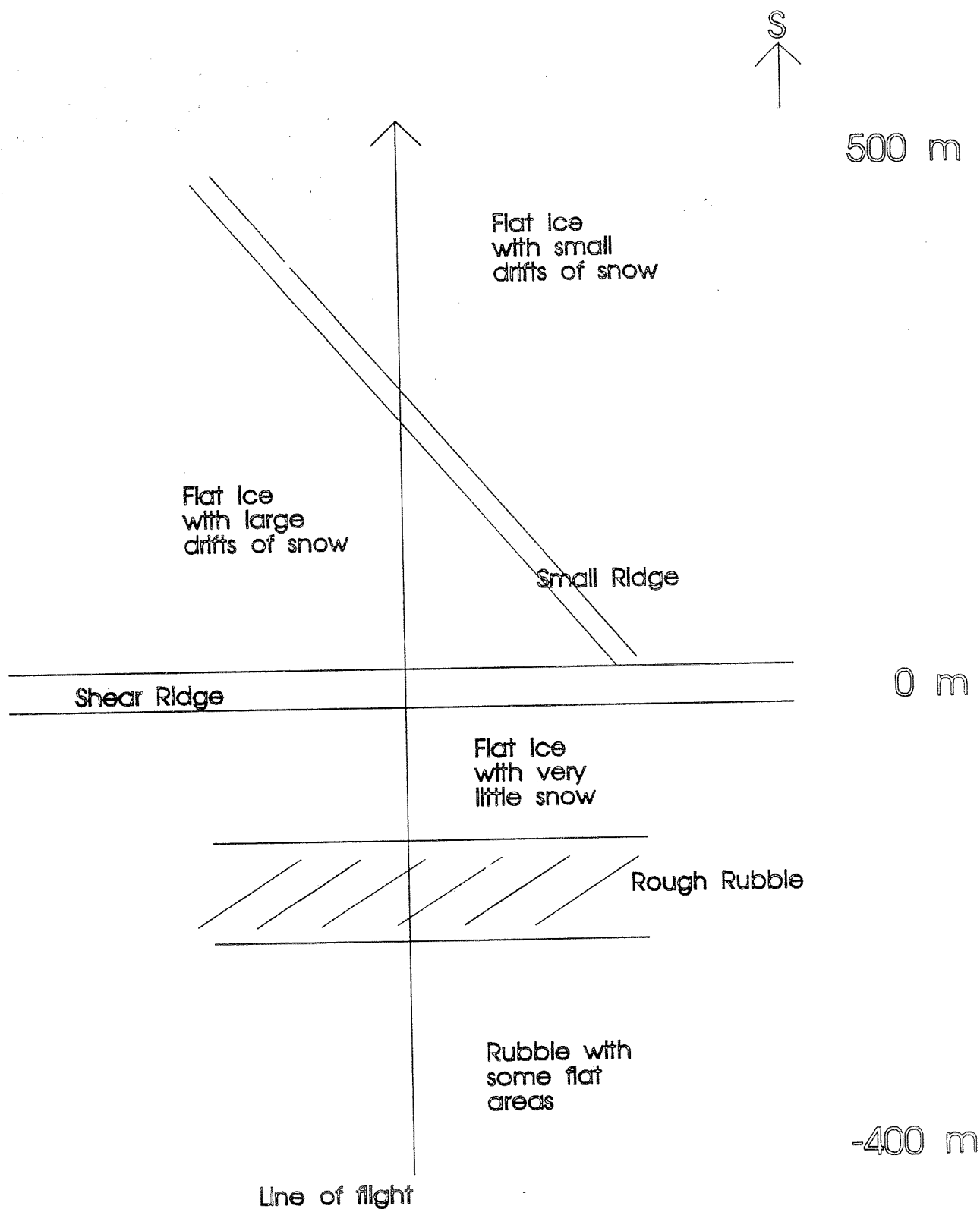


Fig. 3 Sketch of the shear ridge site, with the line direction shown with the arrow.

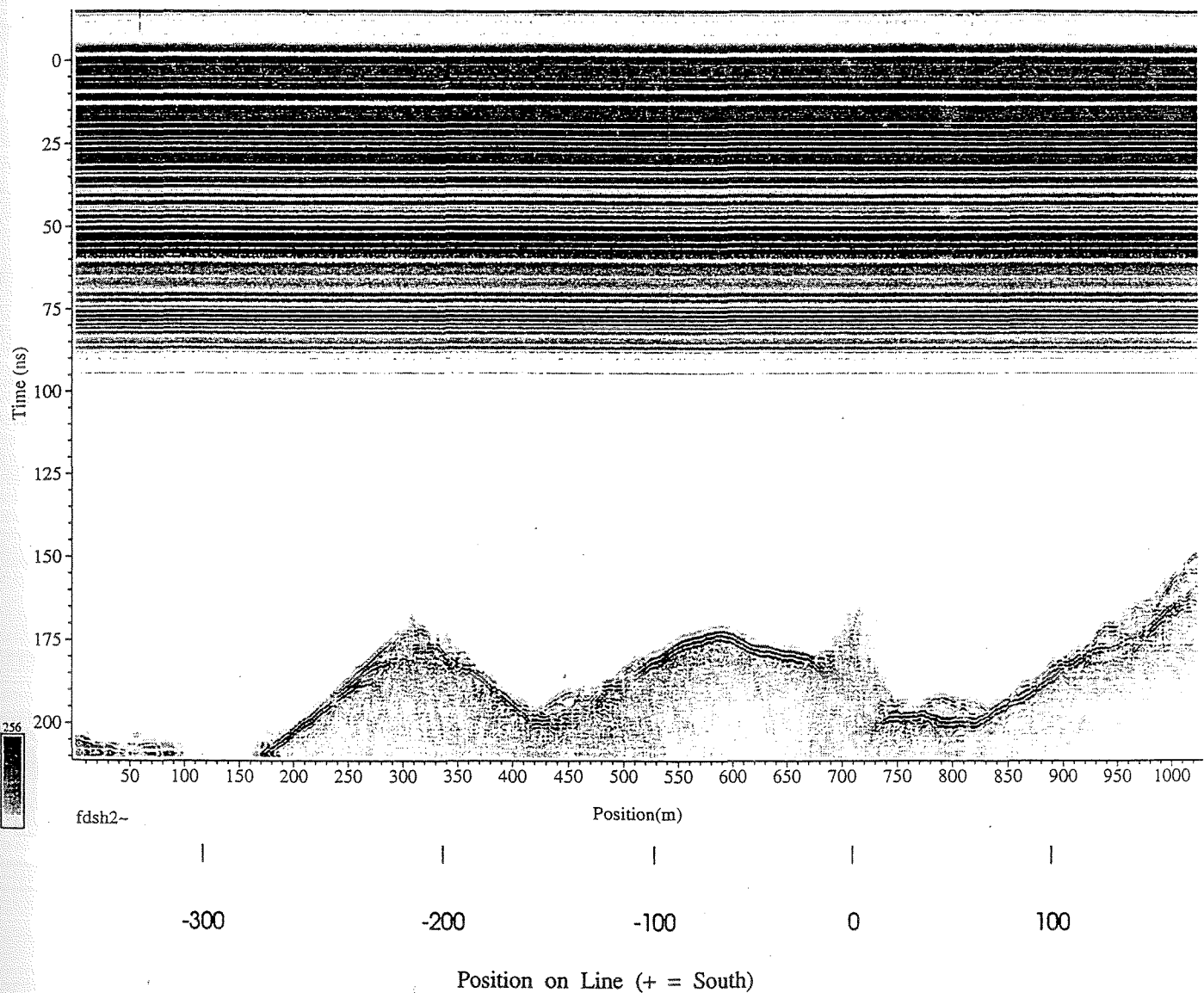


Fig.4 a)

Grey-scale plot of raw radar data from profile SHEAR2 over the shear ridge site, north section, flown April 16, 1991. The vertical axis is two-way travel time of the radar signal in nanoseconds. The horizontal axis is shown with trace numbers and metre position along the line. The height of surface features can be determined using 6.67 ns/m height. Snow thickness can be determined using 13.3 ns/m thickness. For example, the ridge at position 0 was 3 m high and the snow drift at trace number 800 was 0.5 m thick.

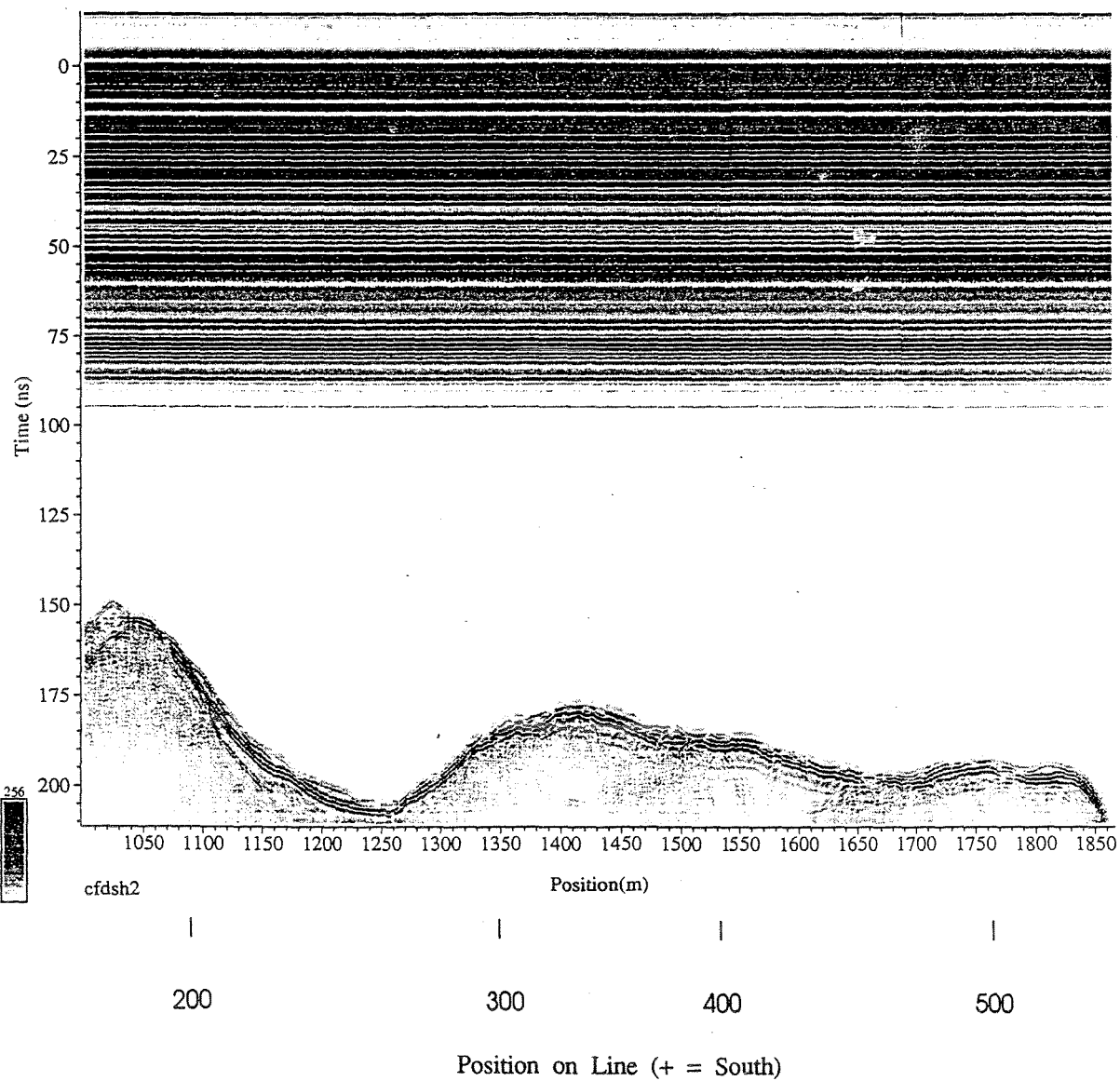


Fig.4 b) Grey-scale plot of raw radar data from profile SHEAR2 over the shear ridge site, south section, flown April 16, 1991. The vertical axis is two-way travel time of the radar signal in nanoseconds. The horizontal axis is shown with trace numbers and metre position along the line. The height of surface features can be determined using 6.67 ns/m height. Snow thickness can be determined using 13.3 ns/m thickness. For example, the ridge at position 0 was 3 m high and the snow drift at trace number 800 was 0.5 m thick.



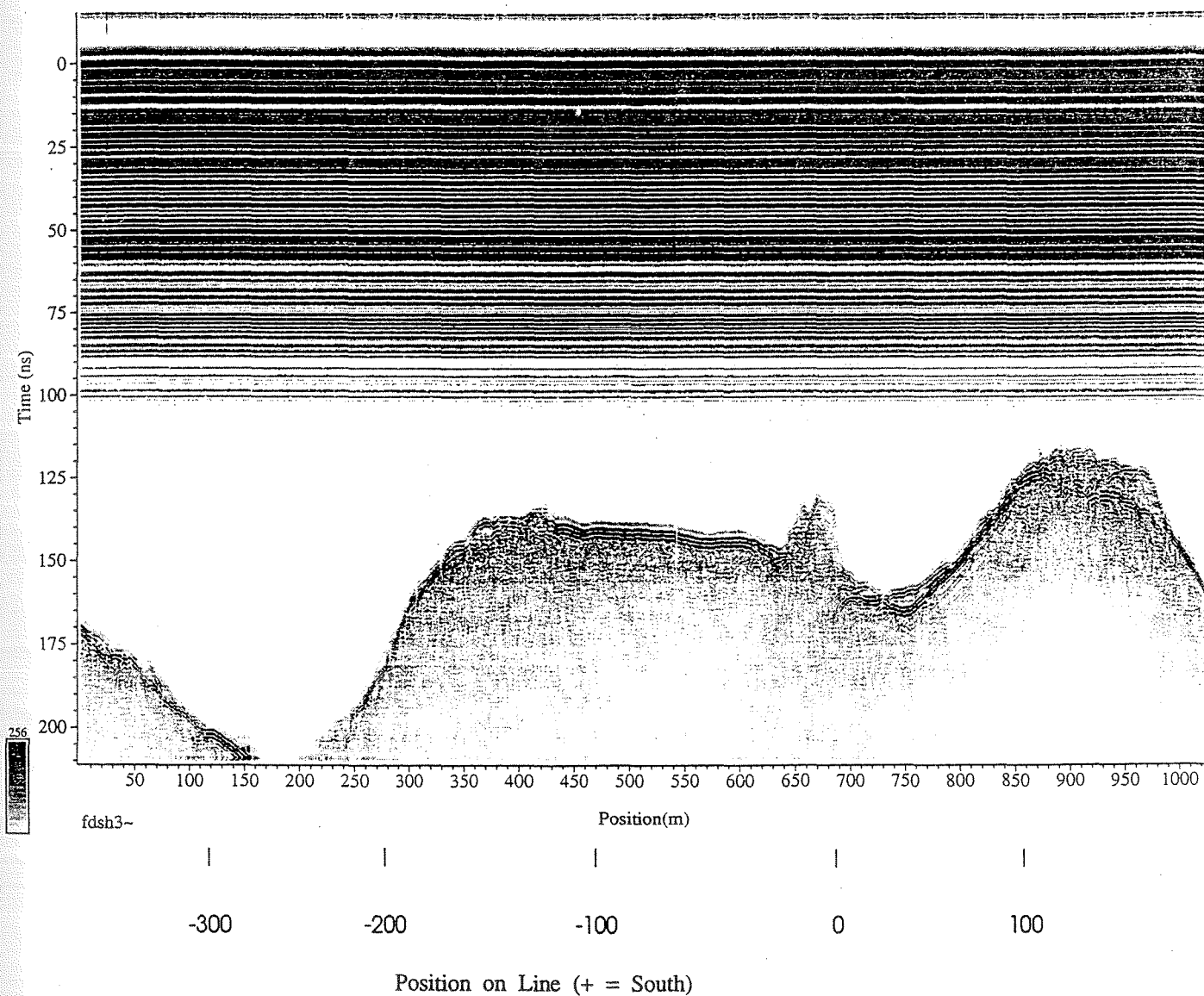


Fig.5 a) Grey-scale plot of raw radar data from profile SHEAR3 over the shear ridge site, north section, flown April 16, 1991. The vertical axis is two-way travel time of the radar signal in nanoseconds. The horizontal axis is shown with trace numbers and metre position along the line.

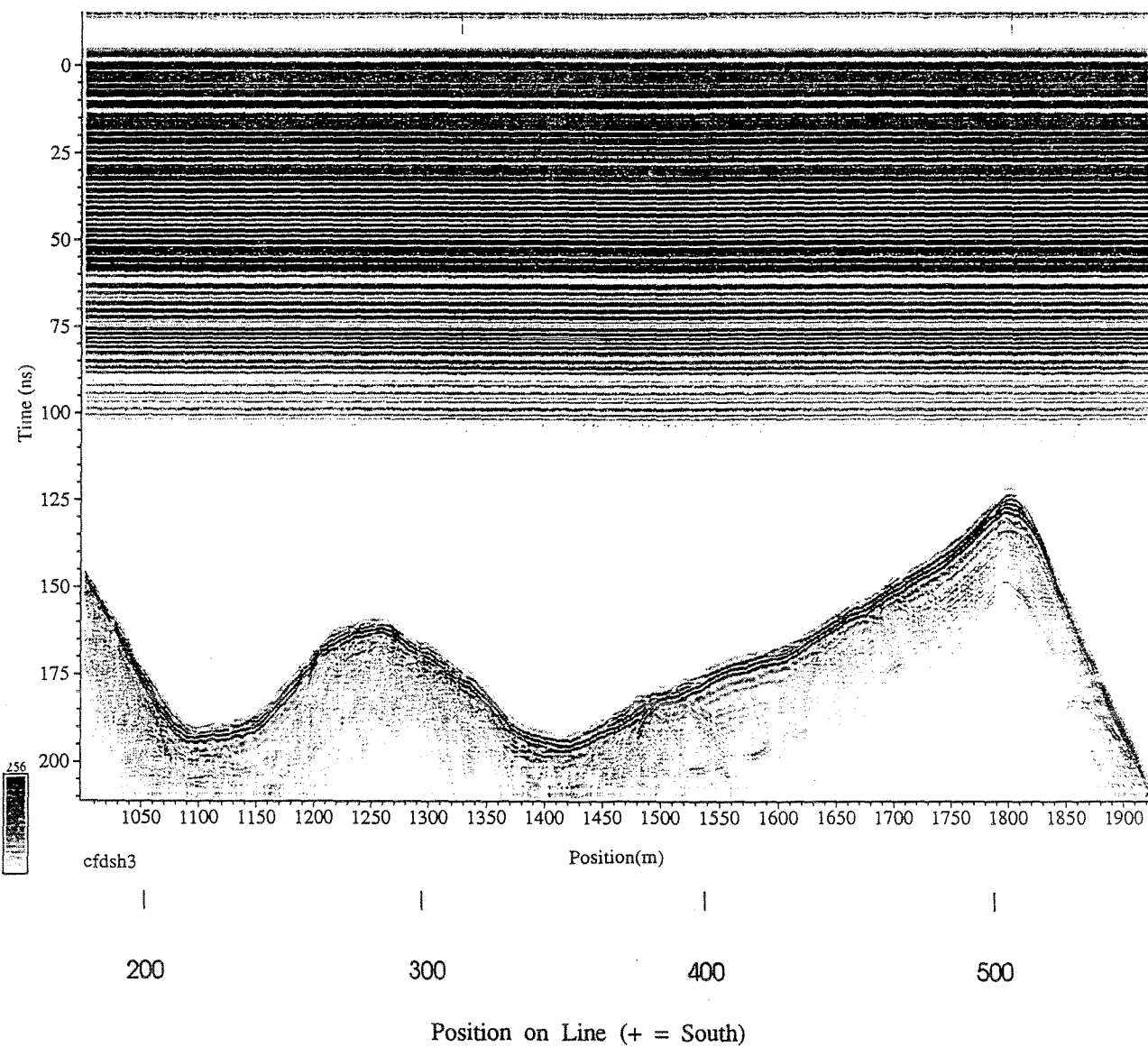


Fig.5 b) Grey-scale plot of raw radar data from profile SHEAR3 over the shear ridge site, south section, flown April 16, 1991. The vertical axis is two-way travel time of the radar signal in nanoseconds. The horizontal axis is shown with trace numbers and metre position along the line.

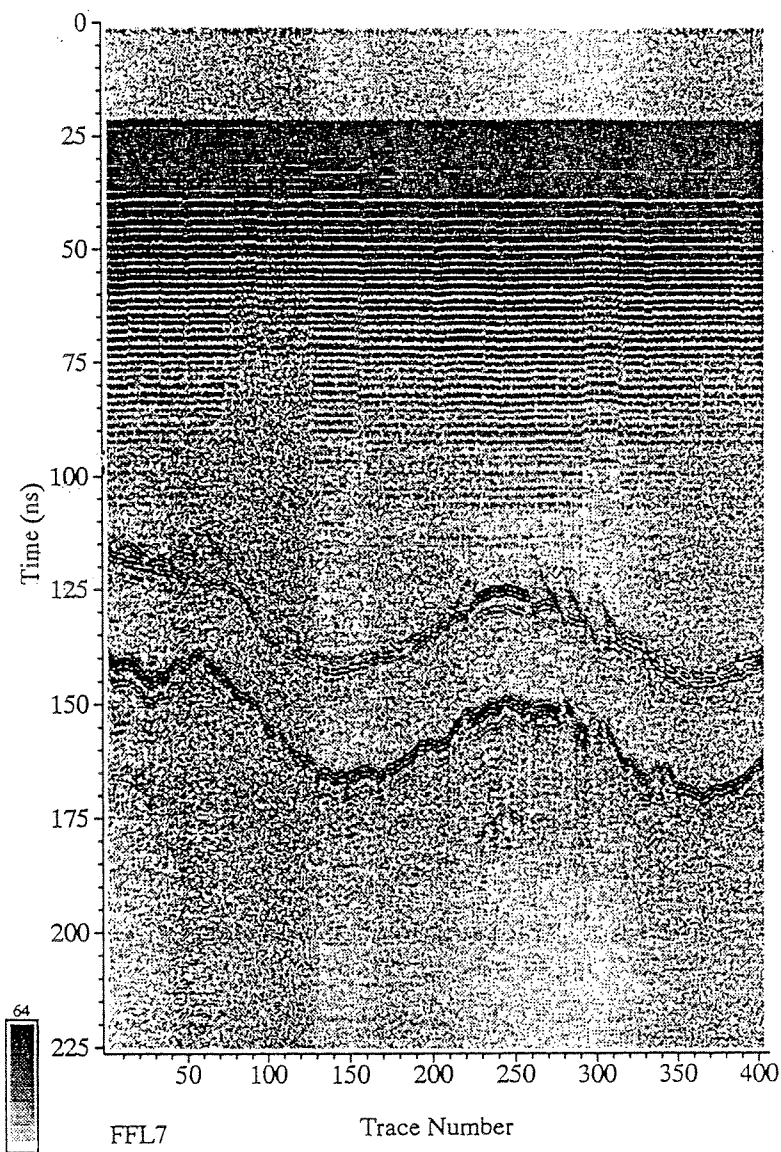


Fig. 6 Grey-scale plot of raw radar data from a profile over the ice road site, flown April 9, 1991. Table 1 lists surface conditions versus trace numbers along the profile. The vertical axis is two-way travel time of the radar signal in nanoseconds. The horizontal axis is trace (scan) number as collected along the profile. Note the echo from the ice/water interface.

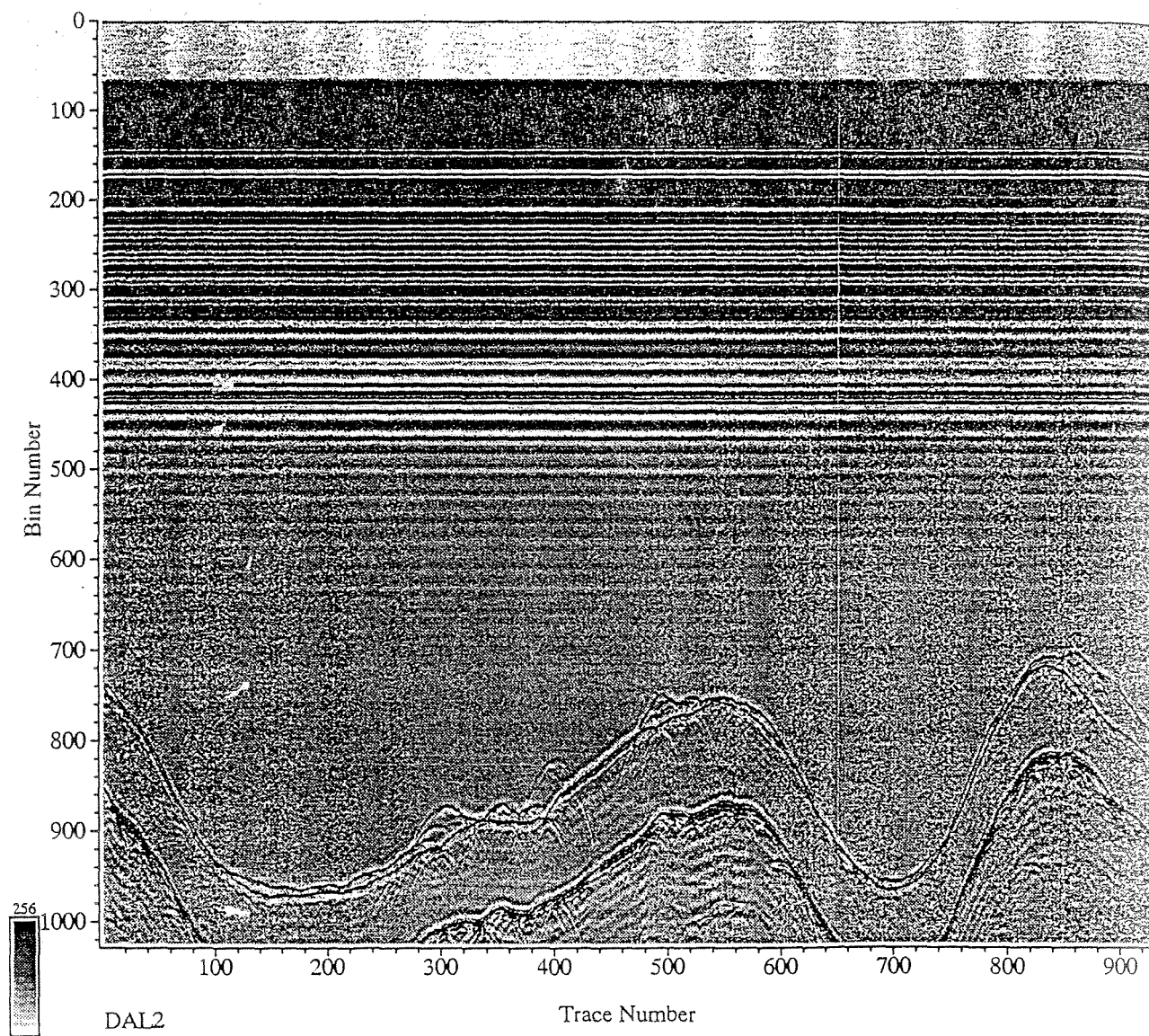


Fig. 7 Grey-scale plot of raw radar data from a profile over the ice road site, flown April 16, 1991. Table 2 lists surface conditions versus trace numbers along the profile. The vertical axis is two-way travel time of the radar signal in nanoseconds. The horizontal axis is trace (scan) number as collected along the profile. Note the echo from the ice/water interface.

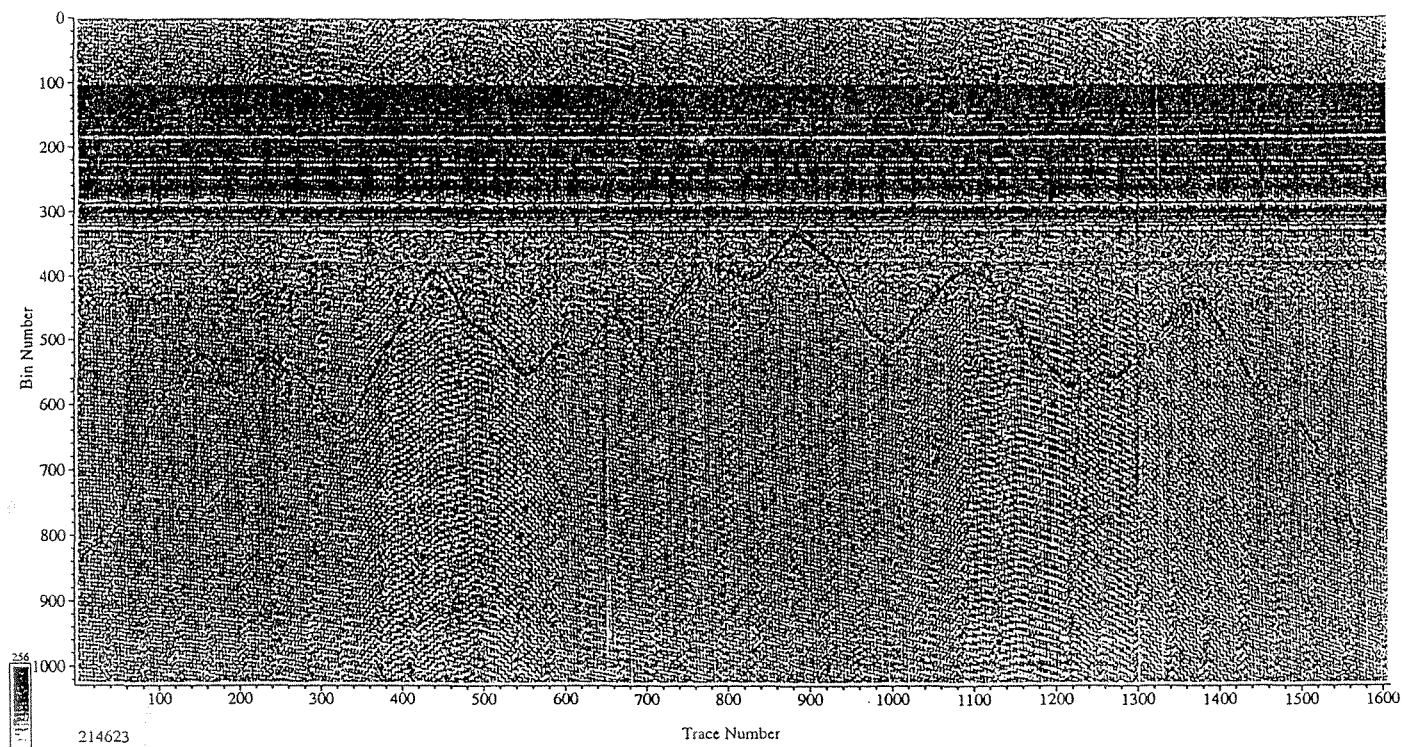


Fig. 8 Grey-scale plot of raw radar data from the profile over the IOS ridge site, flown April 19, 1991. The vertical axis is in number of bins (samples). Each bin represents 0.22 ns in two-way travel time. There is no ground referencing as there was no video imagery for this profile.



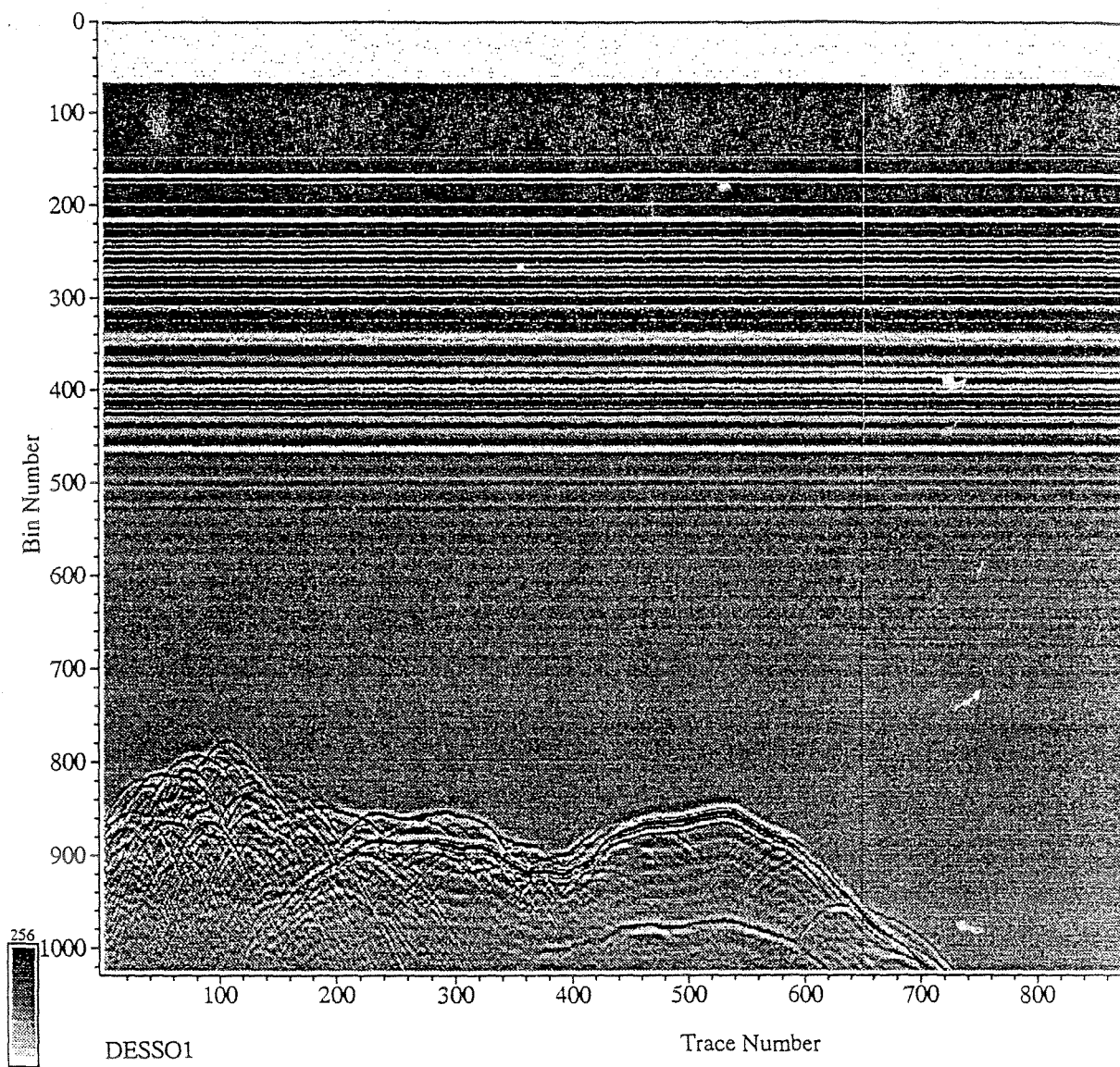


Fig. 9 Grey-scale plot of raw radar data from the profile over the ESSO site, flown April 16, 1991. Table 3 lists surface conditions versus trace numbers along the profile. The vertical axis is two-way travel time of the radar signal in nanoseconds. The horizontal axis is trace (scan) number as collected along the profile.

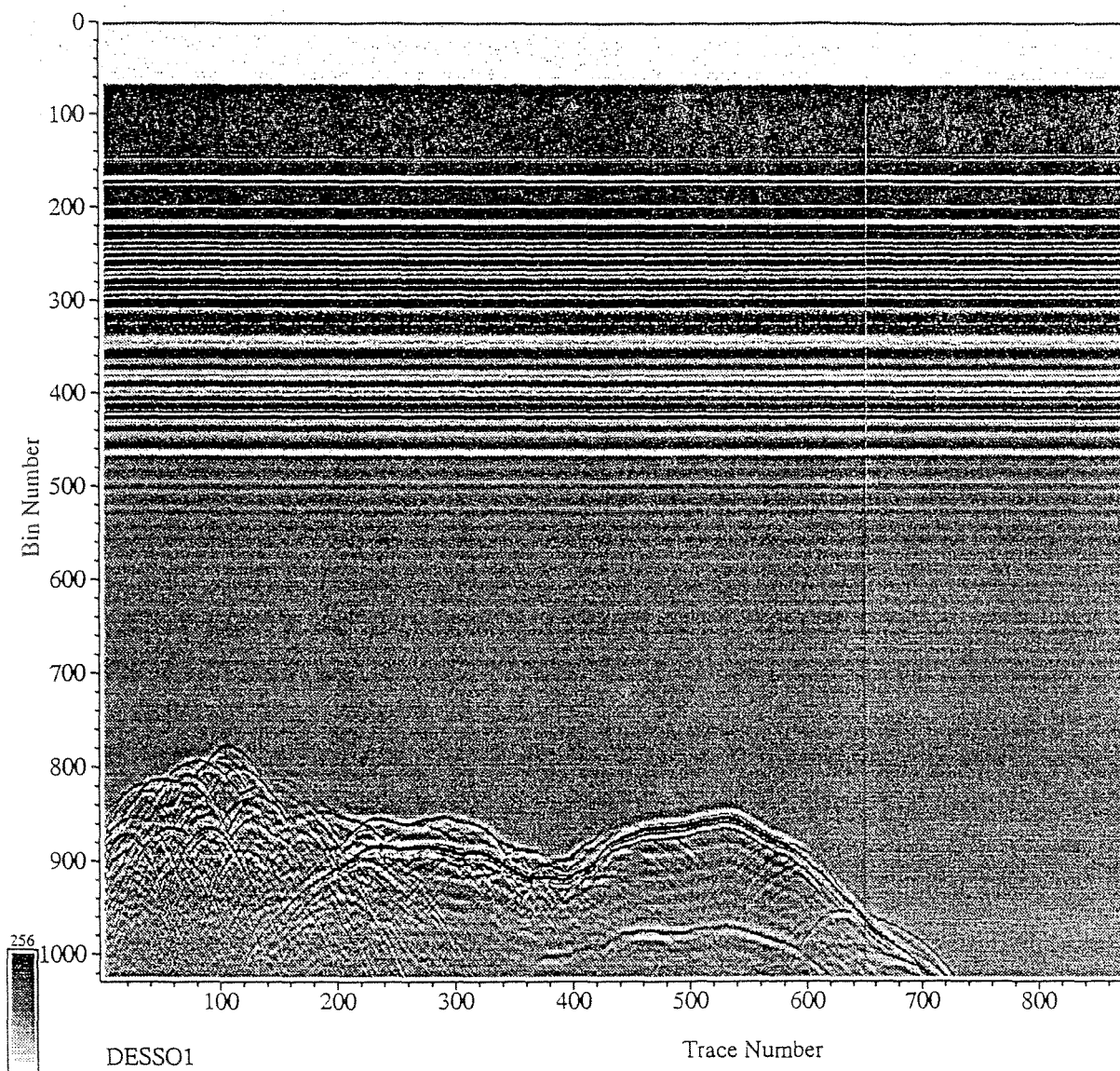


Fig. 9 Grey-scale plot of raw radar data from the profile over the ESSO site, flown April 16, 1991. Table 3 lists surface conditions versus trace numbers along the profile. The vertical axis is two-way travel time of the radar signal in nanoseconds. The horizontal axis is trace (scan) number as collected along the profile.

GPS Flight Paths of 2 Digital Radar Lines  
at Ice Road Site  
(69° N - 133° W)

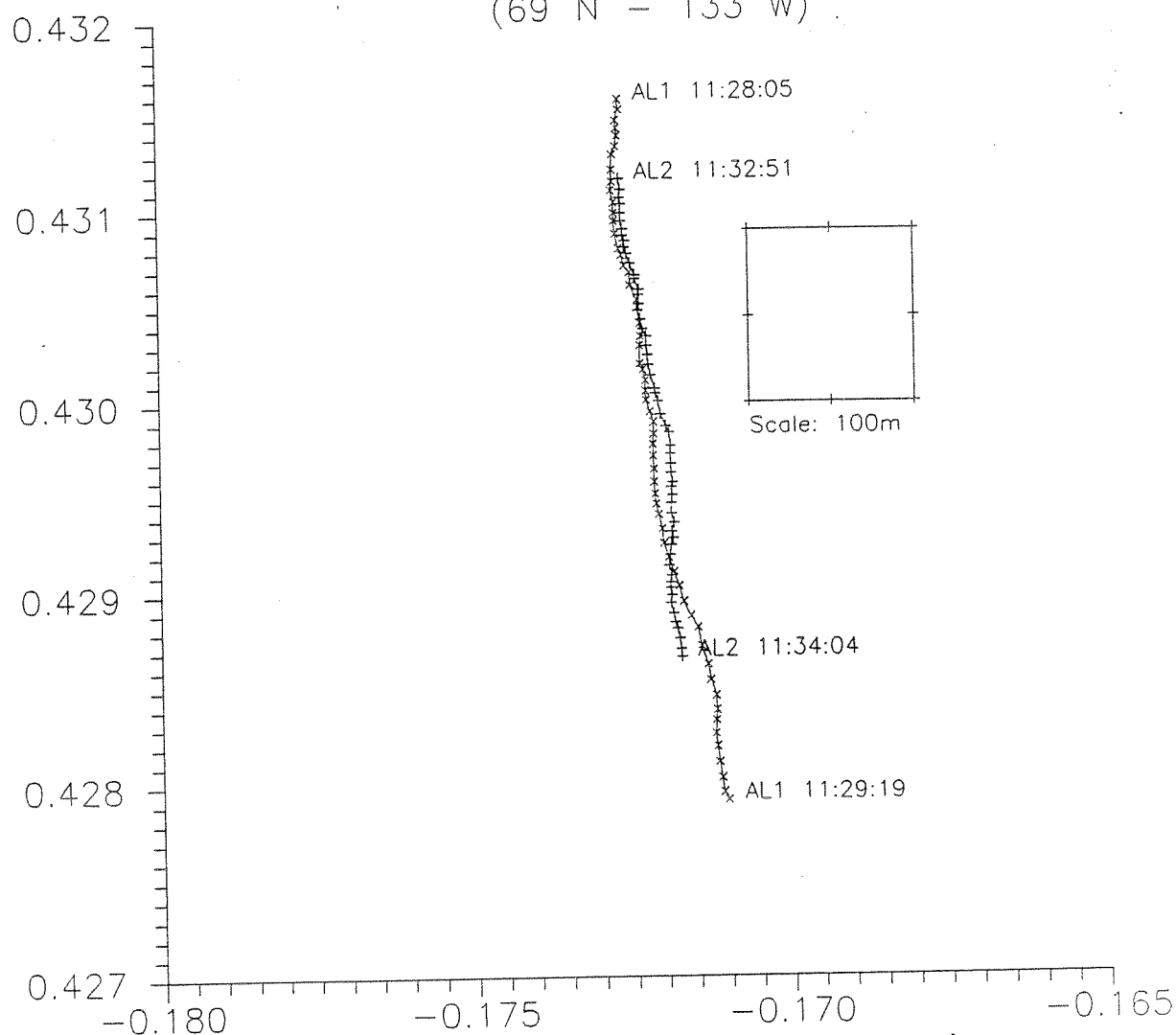


Fig. 10 GPS track plot for 2 profiles over the ice road site, flown April 16, 1991. The vertical axis is decimal degrees north latitude offset from 69° N latitude. The horizontal axis is decimal degrees west longitude offset from 133° W longitude. The track marked AL2 corresponds to the profile plotted in Fig. 7.



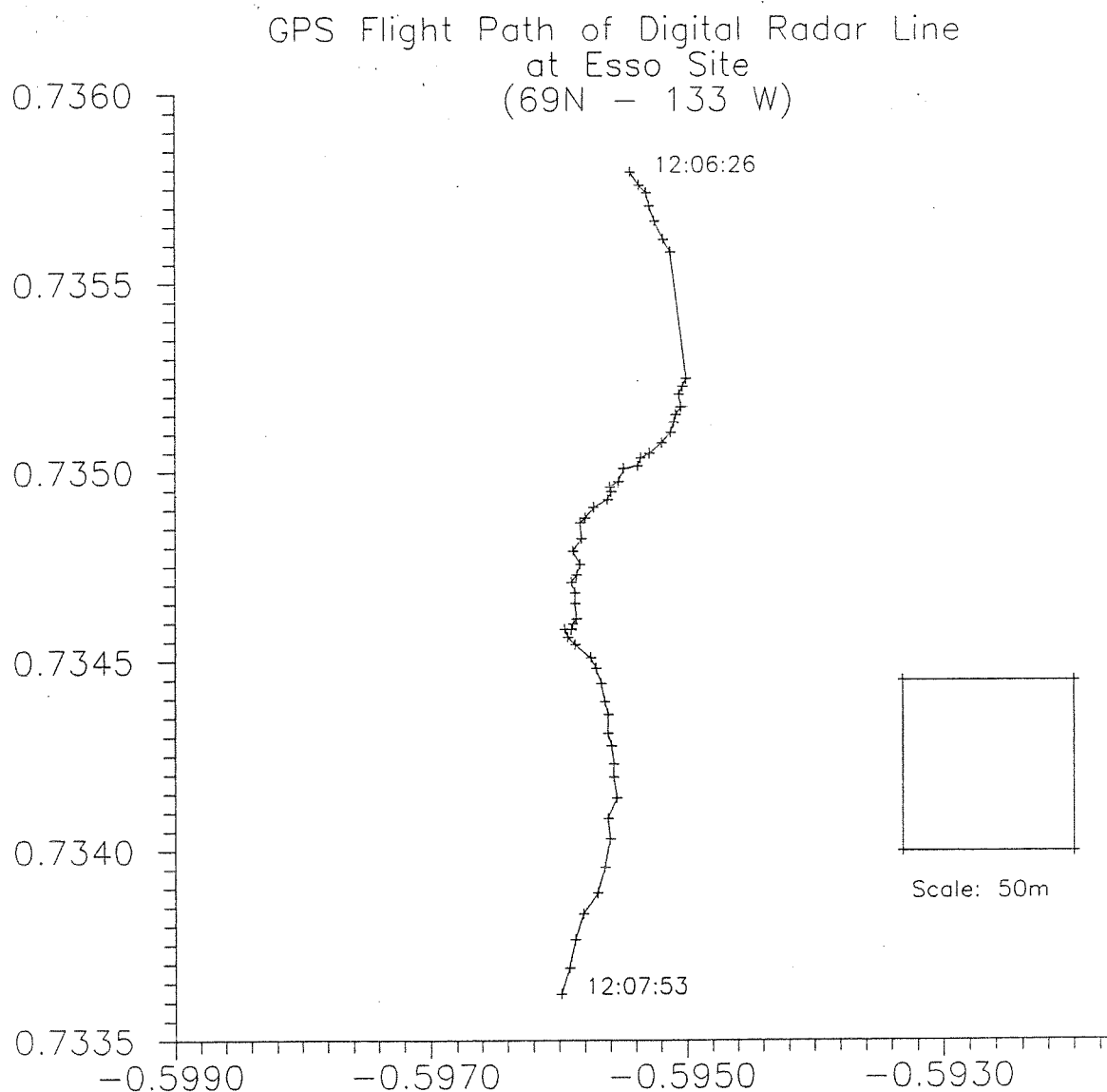


Fig. 11 GPS track plot for the profiles over the ESSO site, flown April 16, 1991. The vertical axis is decimal degrees north latitude offset from 69° N latitude. The horizontal axis is decimal degrees west longitude offset from 133° W longitude. The GPS track corresponds to the profile plotted in Fig. 9.

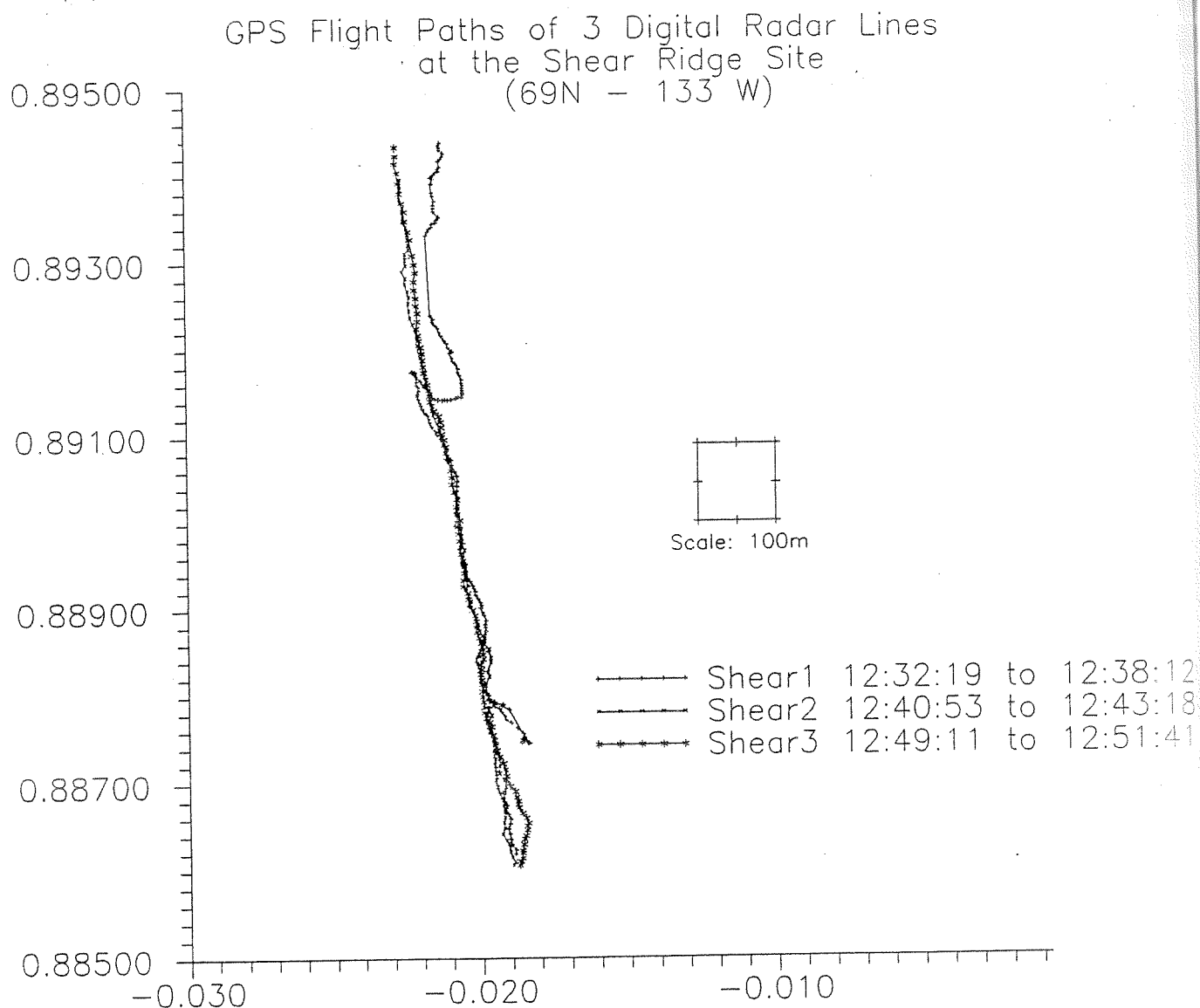


Fig. 12 GPS track plot for the 3 profiles at the shear ridge site, flown April 16, 1991. The vertical axis is decimal degrees north latitude offset from 69° N latitude. The horizontal axis is decimal degrees west longitude offset from 133° W longitude. The radar data for the track marked SHEAR2 is plotted in Fig. 4. The radar data for the track marked SHEAR3 is plotted in Fig. 5.

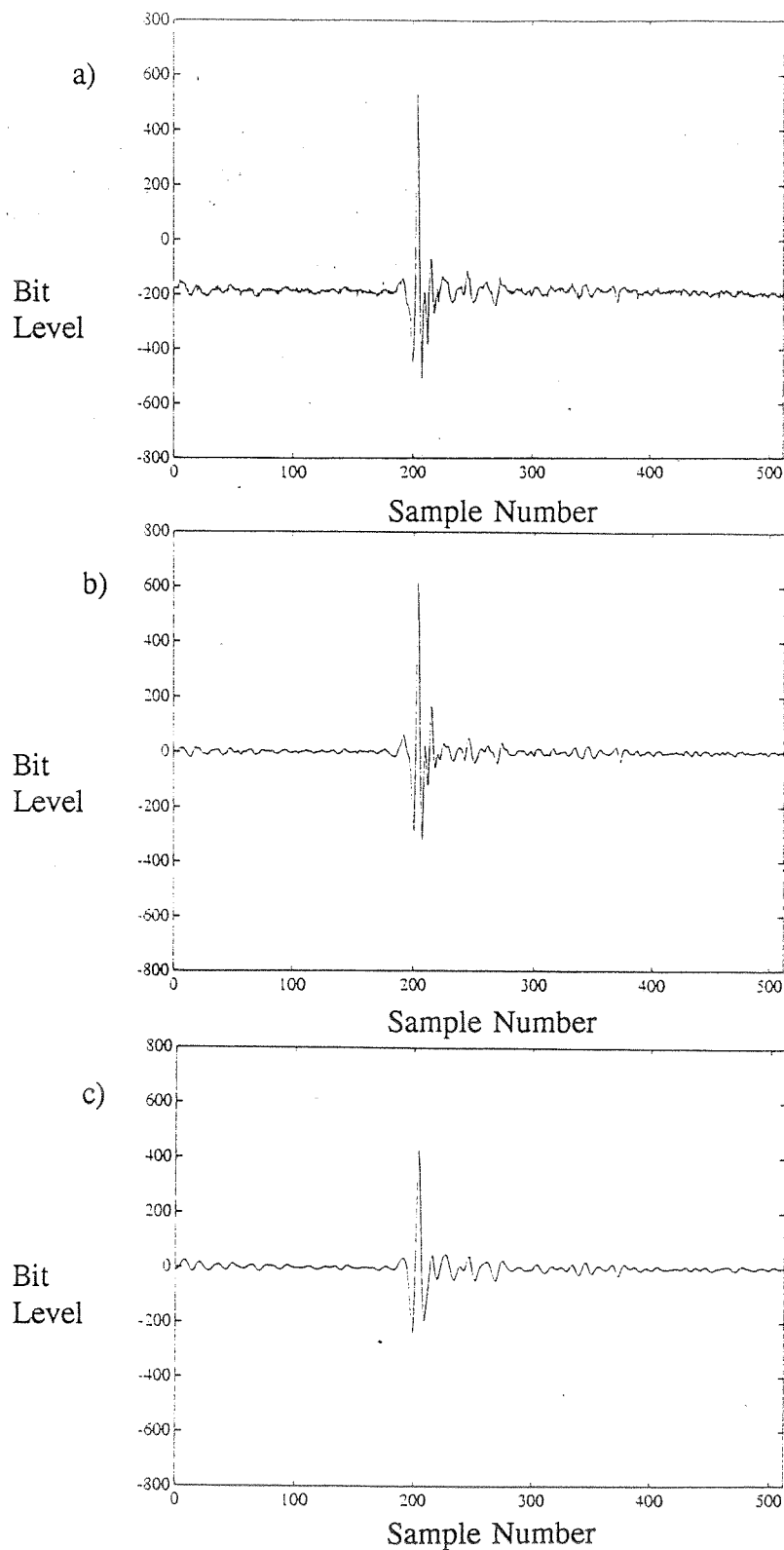


Fig. 13 Oscilloscope plot of the last 512 samples of the first trace from profile SHEAR3.  
a) raw unprocessed data.  
b) band-pass filtered from 250 MHz to 1250 MHz.  
c) band-pass filtered from 125 MHz to 612.5 MHz.

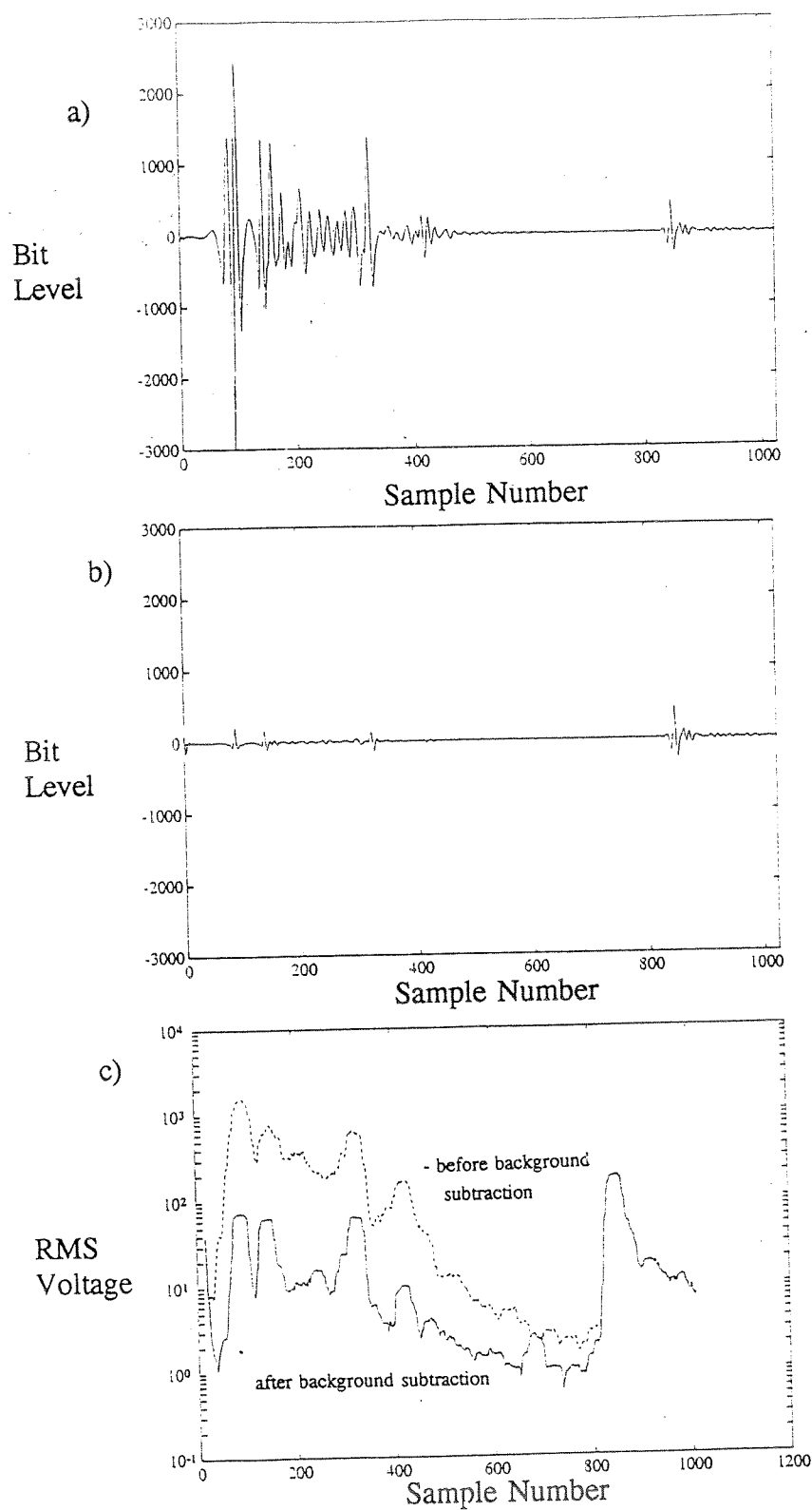


Fig. 14 Results of background subtraction processing on the entire 1024 samples of trace 1 of profile SHEAR3.  
 a) band-passed filtered data (125 MHz to 612.5 MHz).  
 b) Resulting trace after background subtraction.  
 c) RMS voltage levels for traces shown in Fig. 14 a) and 14 b).

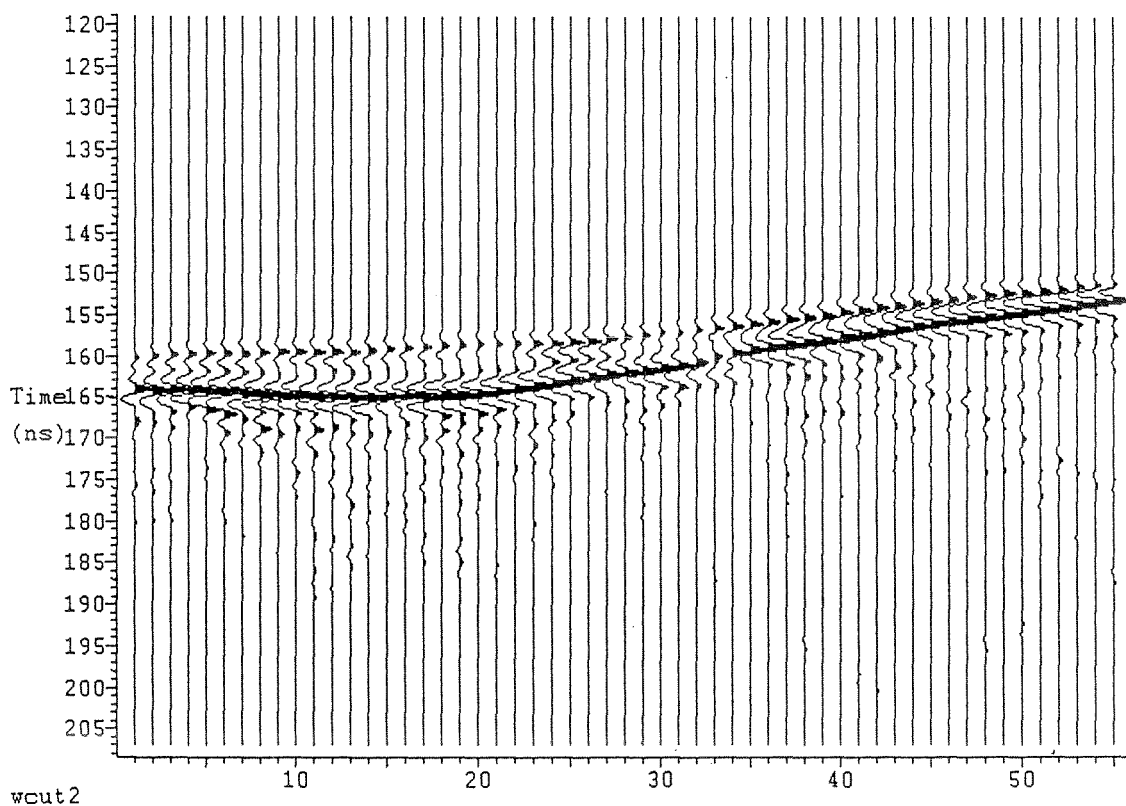


Fig. 15 Variable area plot of radar data from profile SHEAR3, traces 736 to 790. The first echo seen in each trace is from the top of a snow drift. The second echo is a reflection from the snow/ice interface.

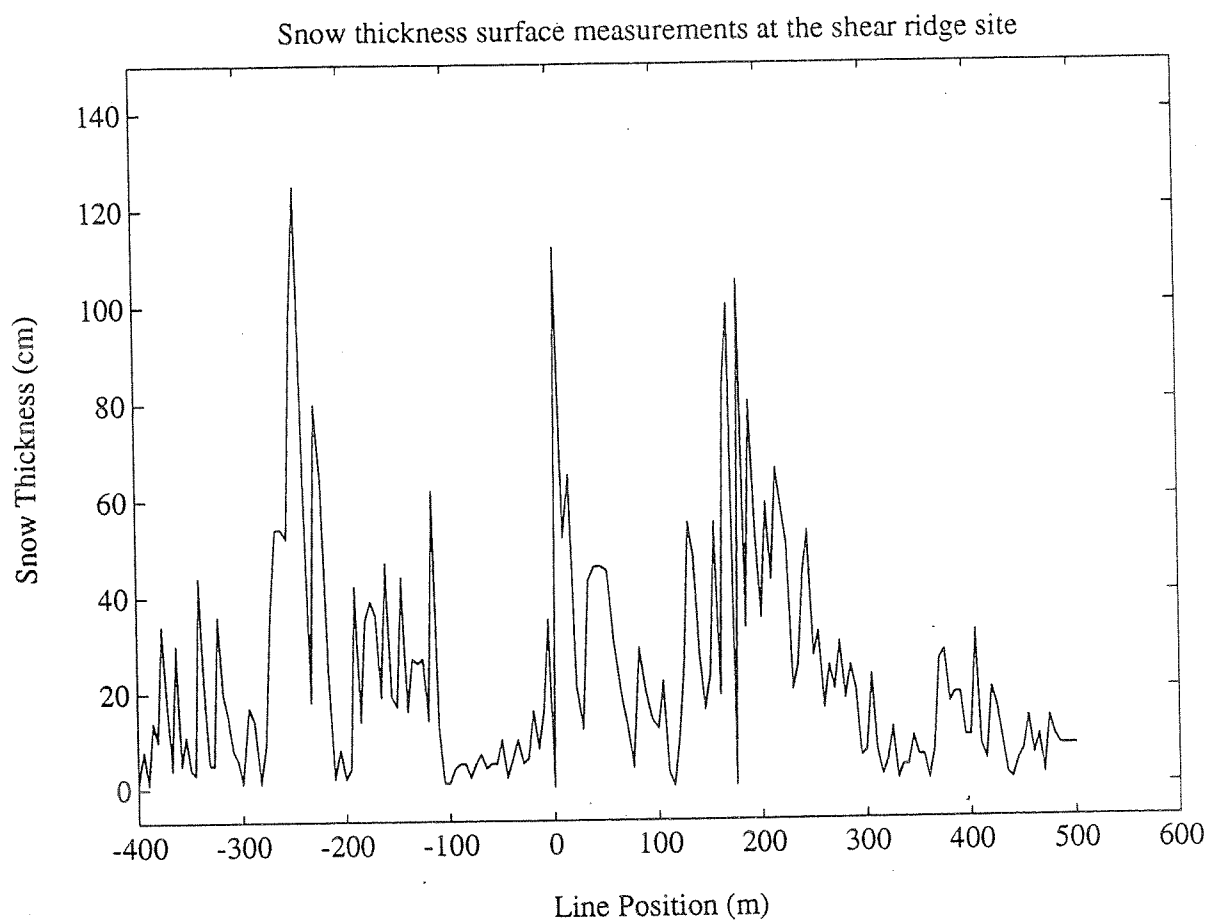


Fig. 16 a) Snow thickness surface measurements taken at the shear ridge site. Measurements were taken at 5 m intervals using a hand probe on April 17, 1991.

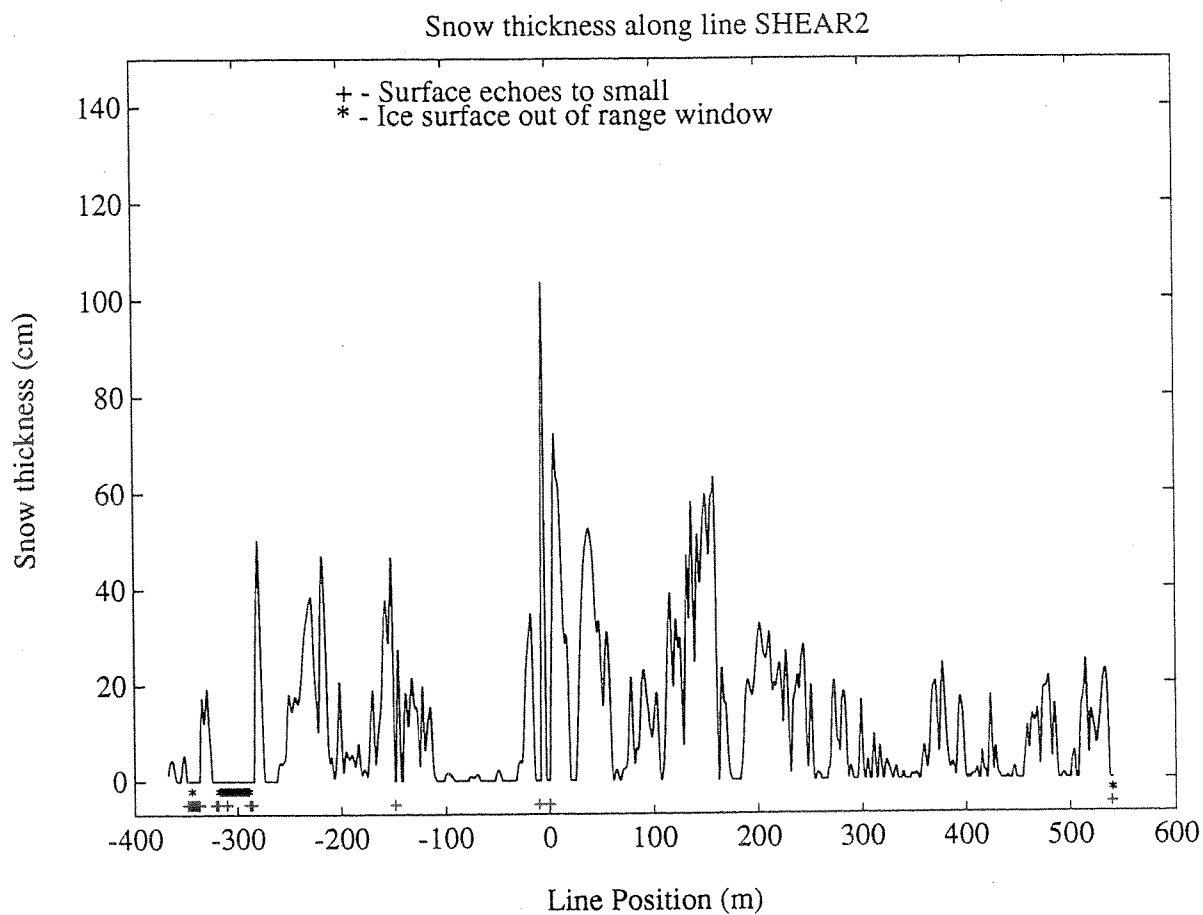


Fig. 16 b) Automated results for the snow thickness radar for profile SHEAR2 at the shear ridge site, flown April 16, 1991.

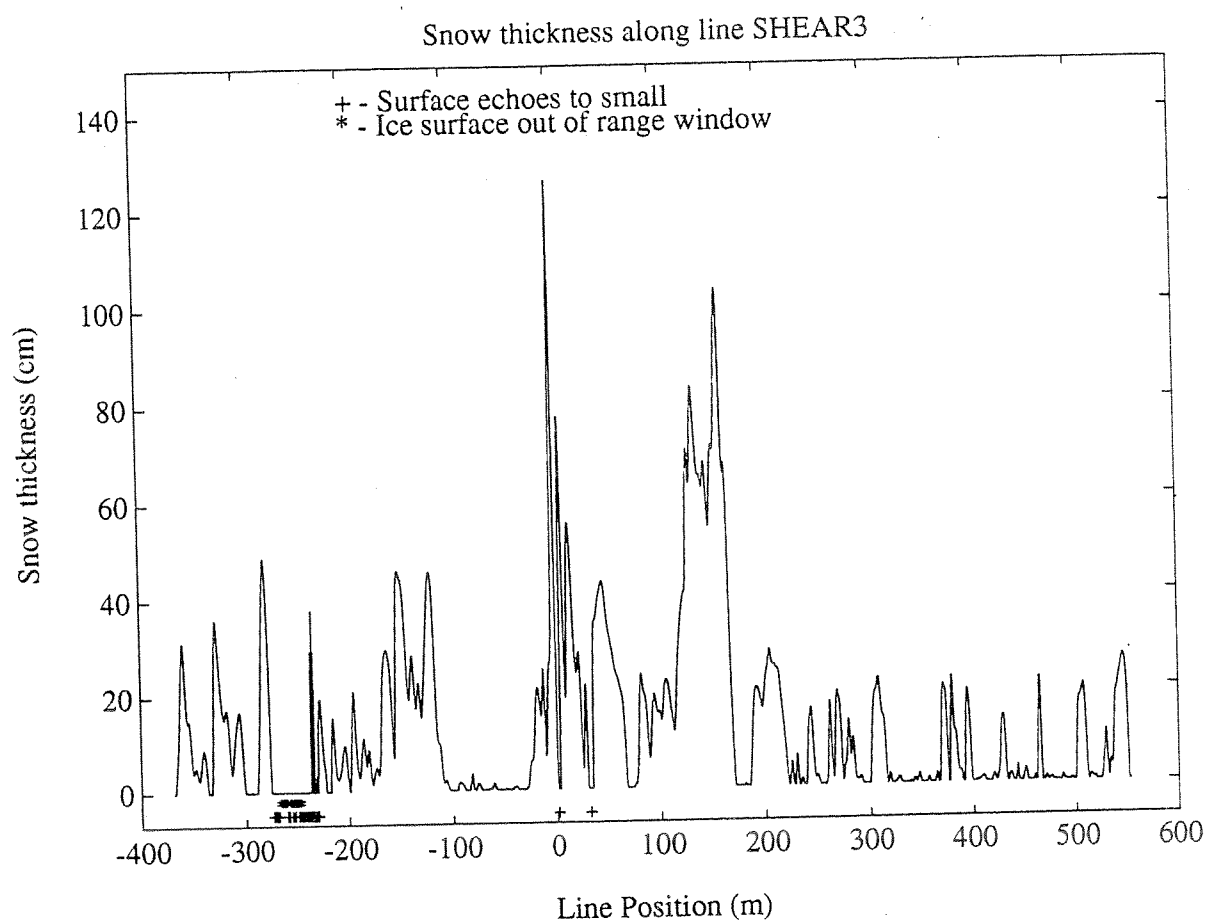


Fig. 16 c) Automated results for the snow thickness radar for profile SHEAR3 at the shear ridge site, flown April 16, 1991.



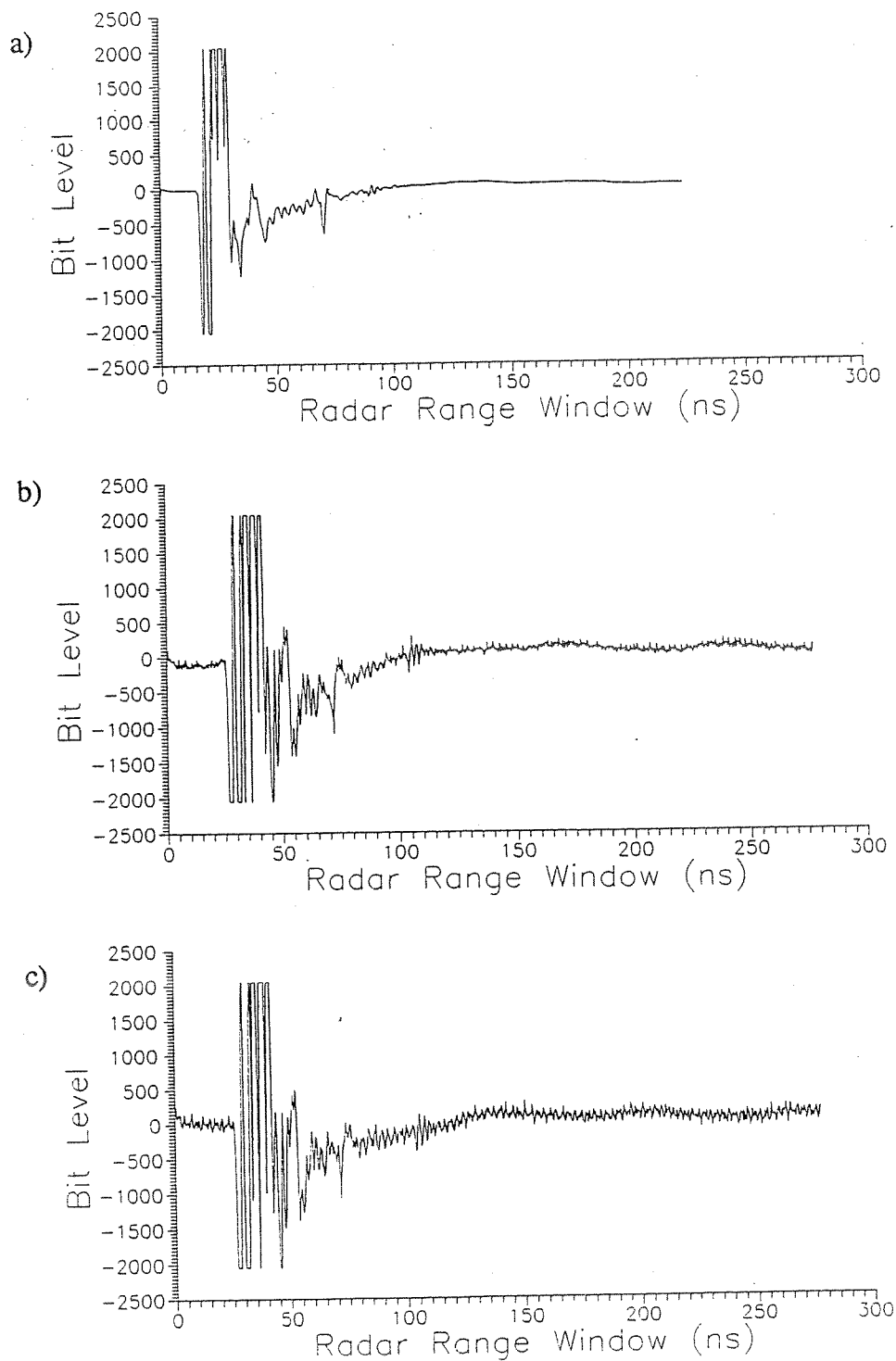


Fig. 17 Noise analysis of radar data when system flown with the EM sensor. Oscilloscope plots individual radar traces.

a) Radar only.

b) EM console turned on, EM transmitters in bird turned off.

c) as b) with EM transmitters in bird turned on.

Power Spectral Density of Radar Data  
with and with-out EM bird

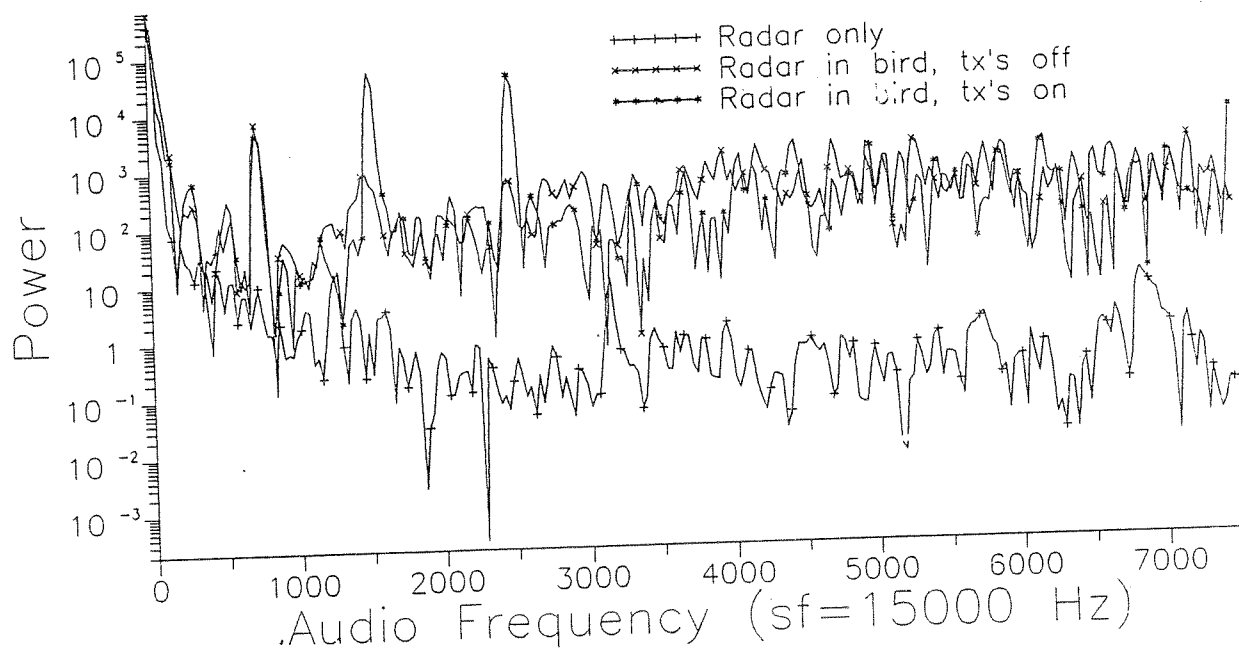


Fig. 18 Power spectral density plots of each trace shown in Fig. 17.

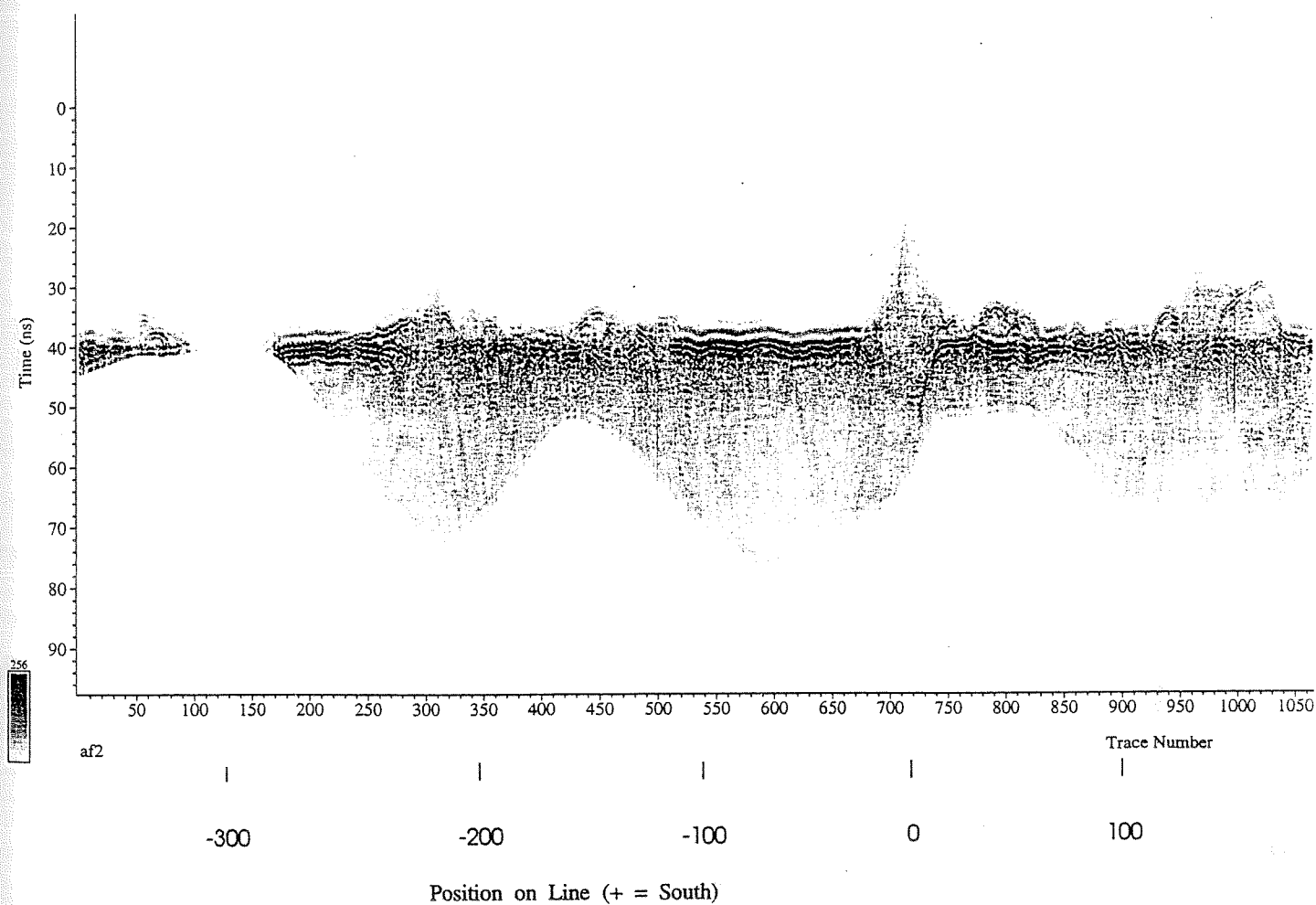


Fig. 19 a) Grey-scale plot of aligned radar data profile SHEAR2 over the shear ridge site, north section. Using results from the snow thickness processing, helicopter height variations have been removed. The vertical axis is two-way travel time in ns, but after alignment processing, only relative time measurements can be made. A plot of the un-aligned data is shown in Fig. 4 a) and b).

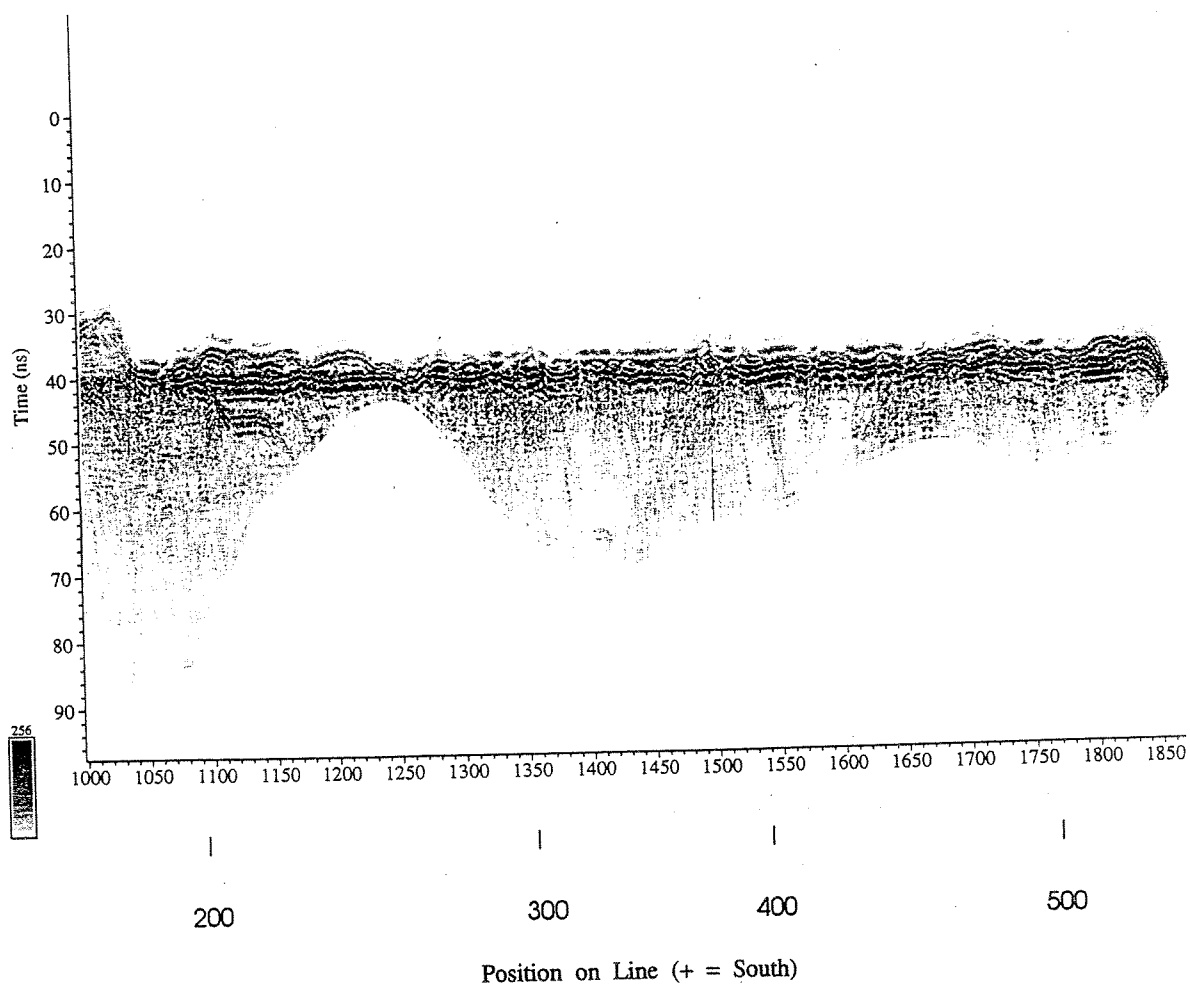


Fig. 19 b) Grey-scale plot of aligned radar data profile SHEAR2 over the shear ridge site, south section. Using results from the snow thickness processing, helicopter height variations have been removed. The vertical axis is two-way travel time in ns, but after alignment processing, only relative time measurements can be made. A plot of the un-aligned data is shown in Fig. 4 a) and b).

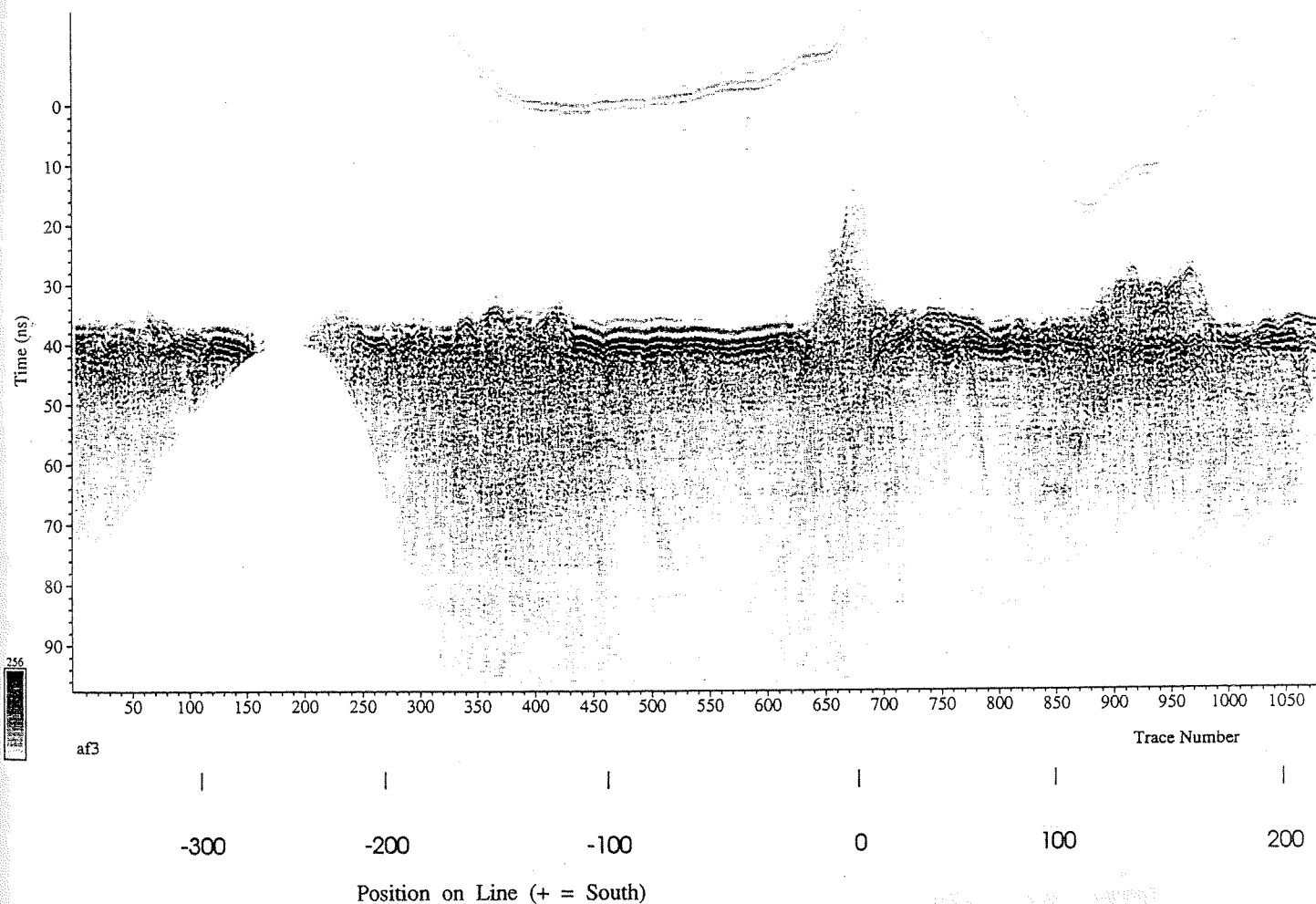


Fig. 20 a) Grey-scale plot of aligned radar data profile SHEAR3 over the shear ridge site, north section. Using results from the snow thickness processing, helicopter height variations have been removed. The vertical axis is two-way travel time in ns, but after alignment processing, only relative time measurements can be made. A plot of the un-aligned data is shown in Fig. 5 a) and b).

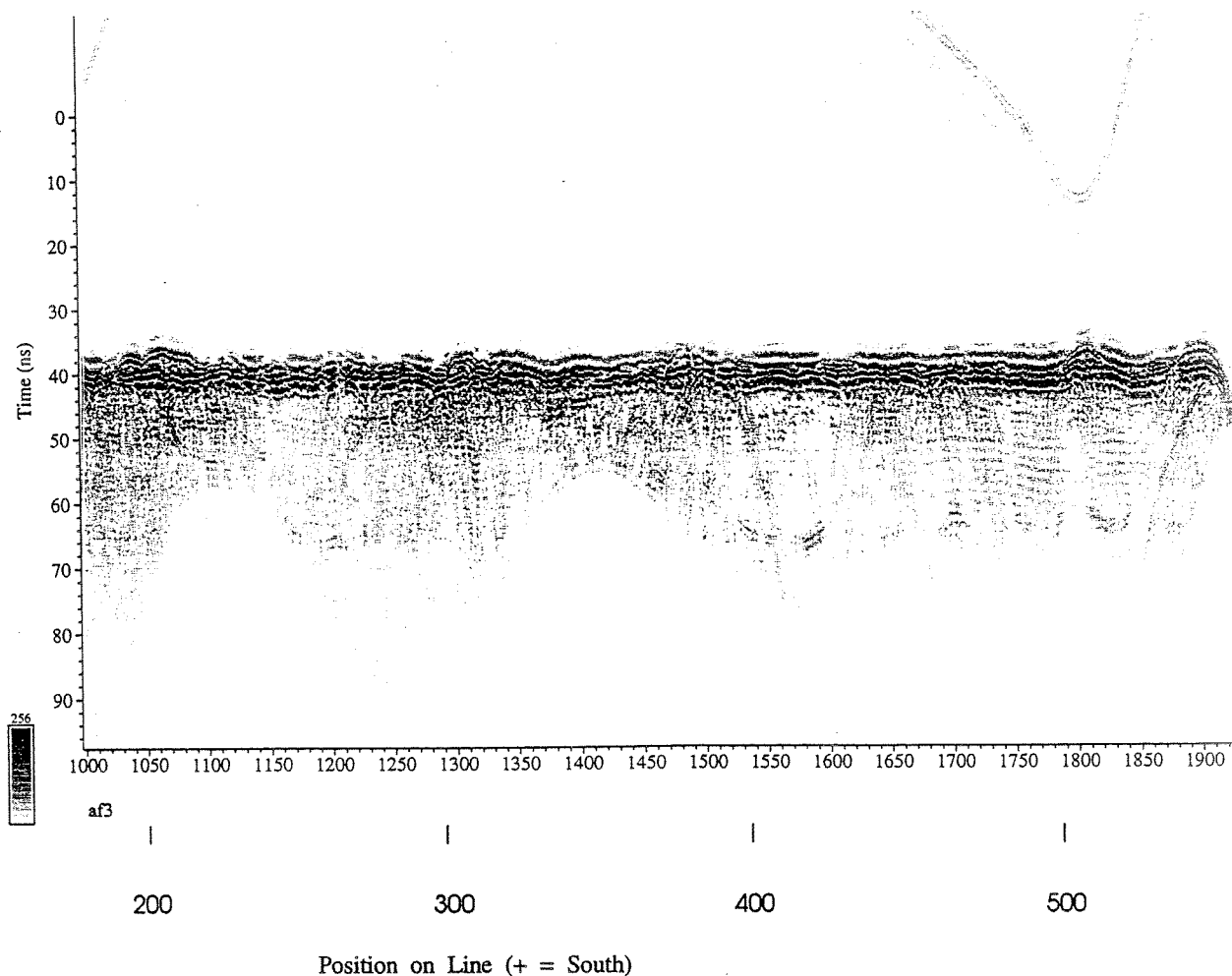


Fig. 20 b) Grey-scale plot of aligned radar data profile SHEAR3 over the shear ridge site, south section. Using results from the snow thickness processing, helicopter height variations have been removed. The vertical axis is two-way travel time in ns, but after alignment processing, only relative time measurements can be made. A plot of the un-aligned data is shown in Fig. 5 a) and b).

## Appendix A: Listing of processing routines

```
function y=calcrms(data,width)
%
% CALCRMS Calculate the rms level in a sliding window down a radar trace
%
% Usage: y = calacrms(data,width)
%
%      data - input radar trace
%      width - width of window over rms measurement is made
%

[m,n]=size(data)
y=zeros(m,n);

for j=1:n

    start=0;           %set up pointers
    fin=width-1;
    mid=width/2;

    while fin<m
        start=start+1;    % slide pointers down trace
        fin=fin+1;
        mid=mid+1;
        y(mid,j)=std(data(start:fin,j)); % use built in standard deviation
                                           % function to approx. rms level.
    end
end
```

```

function y = snthproc(x,bkgd,thresh,startpt)
%
%
% SNTHPROC: takes the input raw data and processes one column at a time
%           first the data is bandpassed filtered
%           then the processed background is subtracted
%           then the column has peaks converted to zero crossings
%           then the zero crossings are detected and its peak value stored
%           then the max peak in the column is located
%           then the first peak over the given threshold is located
%
% Usage y = snthproc(rawdata,bkgdavg,snowthreshold)
%
%       rawdata - snow thickness radar sensor data
%       bkgd - trace used for background subtraction
%       thresh - threshold number used in the detection of snow peaks
%       startpt - bin position where RMS noise level is one tenth threshold
%

[m,n]=size(x);
y=zeros(n,4);

[b,a]=butter(2,[125 612.5]/2.3);           % calculate filter weights for a second
                                           % order filter with a pass band of
                                           % 125 MHz to 612.5 MHz.

for j=1:n
    fprintf('logfile',['count: %6.f',10],j); % record progress in log file
    xj=x(:,j);                             % extract radar trace from matrix
                                           % of data

    xj=filtfilt(b,a,xj);                   % filter trace

    xj=xj-bkgd;                             % subtract background average

    bj=diff4(xj);                          % apply smoothing differentiator

    zj=locpeaks(bj,xj(startpt:n));         % starting from where the noise
                                           % levels are low enough locate
                                           % zero crossing in diff. data
                                           % and extract peak values and
                                           % and peak positions

    [y(j,1) y(j,2)]=max(zj);               % find position and value of
                                           % largest peak

    y(j,3:4)=threspk(zj,thresh);           % find position and value of
                                           % first peak over the threshold
end

```



```

function y = diff4(x)
%
% DIFF4: difference filter with (-1 -1 0 1 1)
%       gives a zero crossing for every peak
%
% Usage: y = diff4(x)
%
%       x - matrix of unsmoothed data
%       y - matrix of differenced data

% Version 1.0
% By: Louis Lalumiere (from Darel Mesher off the Internet)

[m,n]=size(x);
y=zeros(x);

for j=1:n
    for i=3:m-2
        y(i,j)= -x(i-2,j) -x(i-1,j) + x(i+1,j) + x(i+2,j);
    end
end

y=y/4;

```

```

function y = locpeaks(x,Data)
%
% LOCPEAKS: finds zero crossings in differentiated data
%           and puts the peak values into zero crossing
%           location
%
% Usage y = locpeaks(zero crossing_data,pre-processed_data)
%           zero crossing_data - output from DIFF4 processing
%           pre-processed_data - filtered and background subtracted data
%

[m,n]=size(x);
y=zeros(m,n);

for j=1:n
    for i=2:m
        if x(i-1,j) > 0
            if x(i,j) <= 0
                % if data values were positive and
                % are now negative or zero, a zero
                % crossing has occurred.

                y(i,j)=Data(i,j);
                % place peak value at postition of
                % zero crossing.
            end
        else
            if x(i,j) >= 0
                % if data values were negative and
                % are now positive or zero, a zero
                % crossing has occurred.

                y(i,j)=Data(i,j);
                % place peak value at postition of
                % zero crossing.
            end
        end
    end
end
end

```

```

function y = threshpk(x,thresh)
%
% THRESHPK: finds the location of the first peak over
% the threshold, returning the peak value and
% its position.
%
% Usage y = threshpk(pre-processed_data,threshold)
%
% pre-processed_data - filtered and background subtracted data
% threshold - threshold number used for the detection
% of possible snow peaks
%

[m,n]=size(x);
y = zeros(n,2);

for j=1:n
    i=1;
    while x(i,j) < thresh % step down trace until values no longer
                        % less than threshold

        i=i+1;
        if i>m % if no value found in trace greater than
            i=m; % threshold then position return is set to the
                % last trace position

        break;
    end
    end
    y(j,1)=x(i,j); % assign output array with value and
    y(j,2)=i; % location of first position over threshold
end

```

```

function y = snowth(orgdata,thresh,noise)
%
% SNOWTH: takes the difference between the ice peak location
%         and the snow peak location then check to see whether
%         the ice peak value is less than a threshold for ice.
%
% Usage y = snowth([icevalue iceposition snowvalue snowposition],thres,noise)
%
%         icevalue - array of ice peak values
%         iceposition - array of ice peak locations
%         snowvalue - array of snow peak values
%         snowposition - array of snow peak locations
%         thres - threshold number used in the detection of snow peaks
%         noise - noise floor value to de-classify possible ice peaks
%

[m,n]=size(orgdata);
y=zeros(m,3);

[bi ai]=butter(3,.05);      % filter weights to smooth ice peak locations
[bs as]=butter(3,.2);      % filter weights to smooth snow peak locations

fi=filtfilt(bi,ai,orgdata(:,3)); % smooth ice peak locations
fs=filtfilt(bs,as,orgdata(:,5)); % smooth snow peak locations

for j=1:m
% determine flags

    flag =0;

    if (orgdata(j,5)==512 & orgdata(j,2) < noise) % no snow peak found
        y(j,1)=0; % and max peak is in the noise
        y(j,2)=1; % flag that no peak found
        flag=1;
    end

    if (orgdata(j,2) < thresh & orgdata(j,2) >= noise)
        %ice peak value less than threshold for snow
        y(j,1)=0;
        y(j,3)=1; % flag that ice peak to small
        flag=1;
    end

    if orgdata(j,2)/orgdata(j,4) < .99 % if ice and snow position roughly
        y(j,1)=0; % the same.
        flag=1;
    end

% calculate snow thickness in bins

    if flag == 0
        y(j,1)=fi(1) - fs(j);
        if y(j,1) < 0
            -y(j,1)=0;
        end
    end
end
end

```

```

function y = icealign(data,offset)
%
% ICEALIGN: move traces in profile down for positive offset
%           and up for negative offset. Offset based on position of
%           ice surface determined during snow thickness processing.
%
%           The routine GETALIGN condition the ice peak data to provide
%           The offset information.
%
% Usage:      y = align(data,offset);
%
%           data - matrix with one or more columns of data
%           offset - array of offset information
%           y - matrix of aligned data
%
% Version 1.0
% By: Louis Lalumiere

[m,n]=size(data);
y=zeros(m,n);

halfpt = m/2;

for i=1:n
    offs= halfpt-offset(i);           % reference ice surface to middle of trace.
    yi=zeros(m,1);
    if offs <= 0                       % if offset less than or equal to zero, set
        newstart = 1;                % set pointers to move data up.
        newfinish = m + offs;
        oldstart = abs(offs)+1;
        oldfinish = m;
    else                               % if offset greater than zero, set pointers
        newstart = offs + 1;          % to move data down.
        newfinish = m;
        oldstart = 1;
        oldfinish = m - offs;
    end

    yi(newstart:newfinish)=data(oldstart:oldfinish,i); % move data in trace.
    y(:,i)=yi;                               % put resulting trace
                                           % into output matrix.
end

```

```

function y = getalign(ice,snow)
%
% GETALIGN: using the detected positions for the snow and ice echos,
%           finds the lower of the two values.
%
% Usage:    y = getalign(ice,snow);
%
n=max(size(ice))
y=zeros(n,1);
for i=1:n
    if ice(i) > snow(i)
        y(i) = ice(i);
    else
        y(i) = snow(i);
    end
end
end

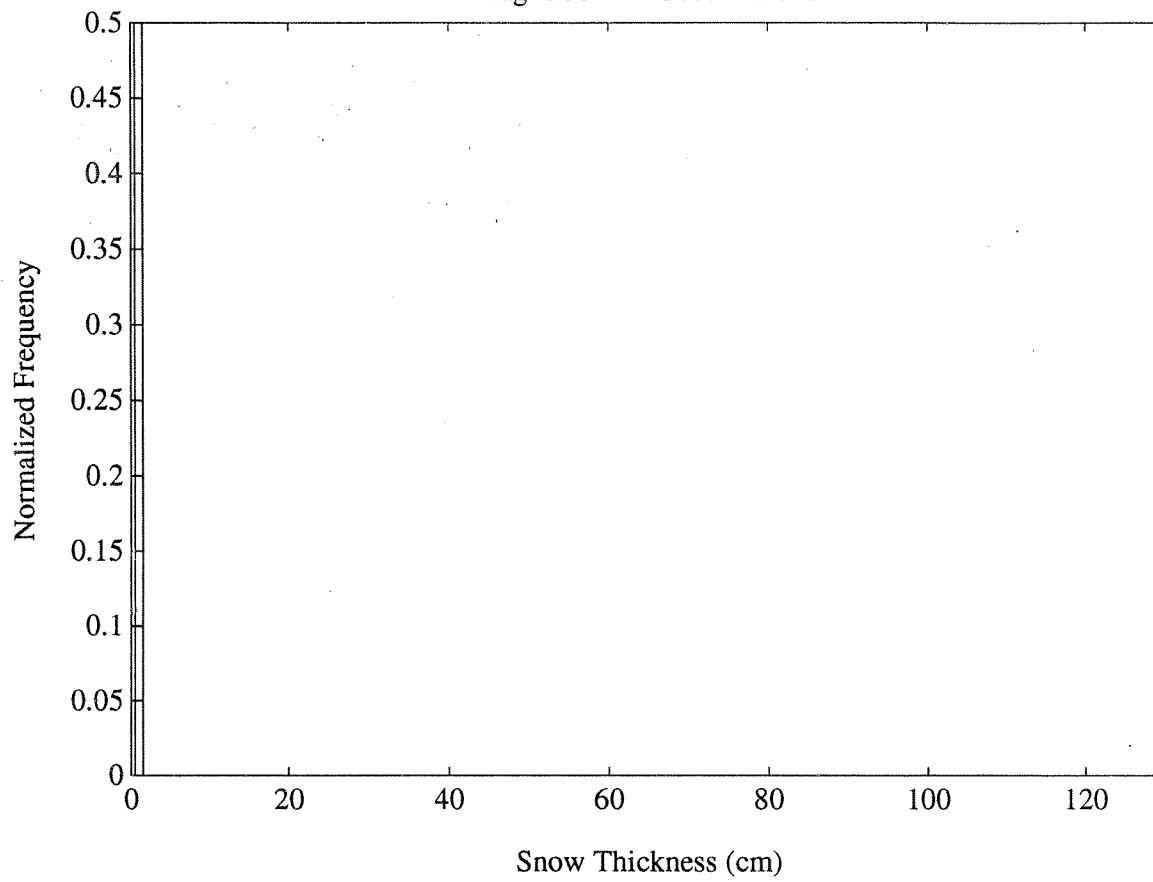
```

**Appendix B: Histograms of snow thickness at marker positions for lines SHEAR2 and SHEAR3**

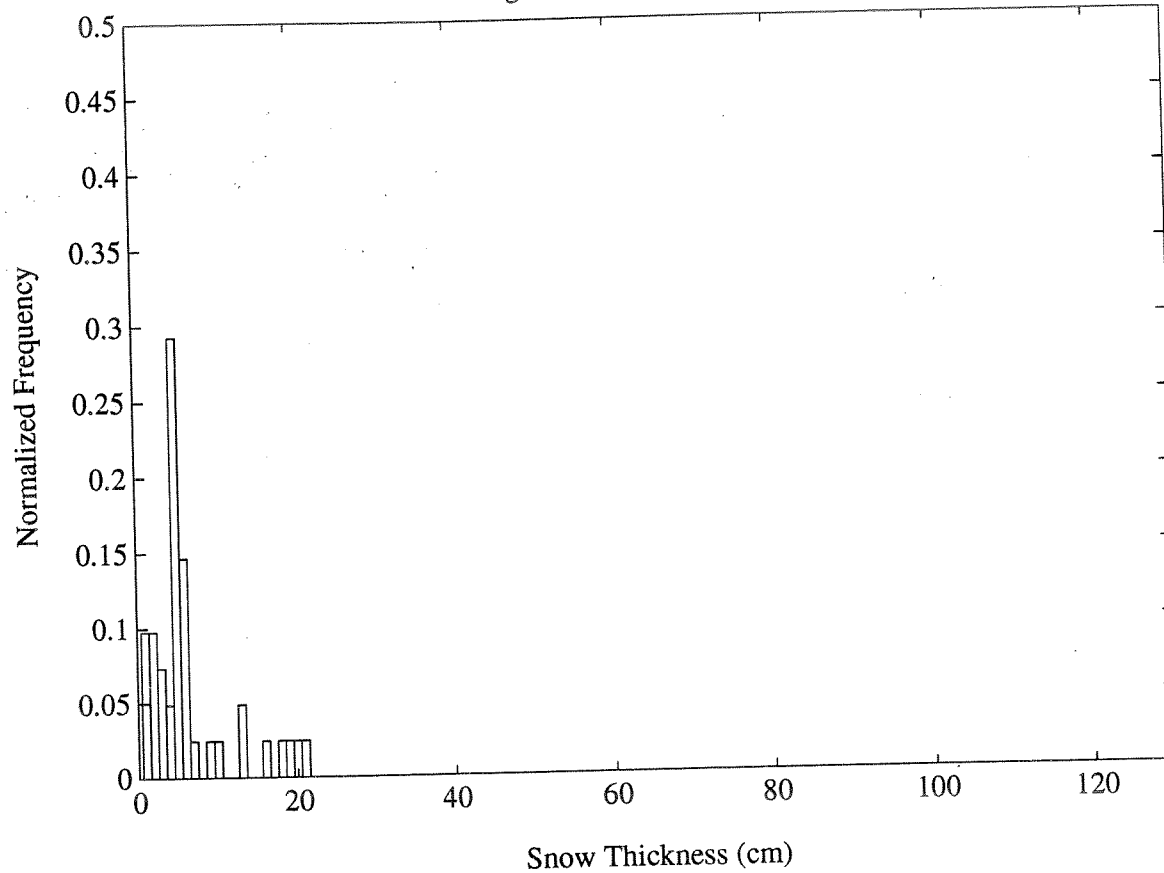
**Histograms for line SHEAR2.**

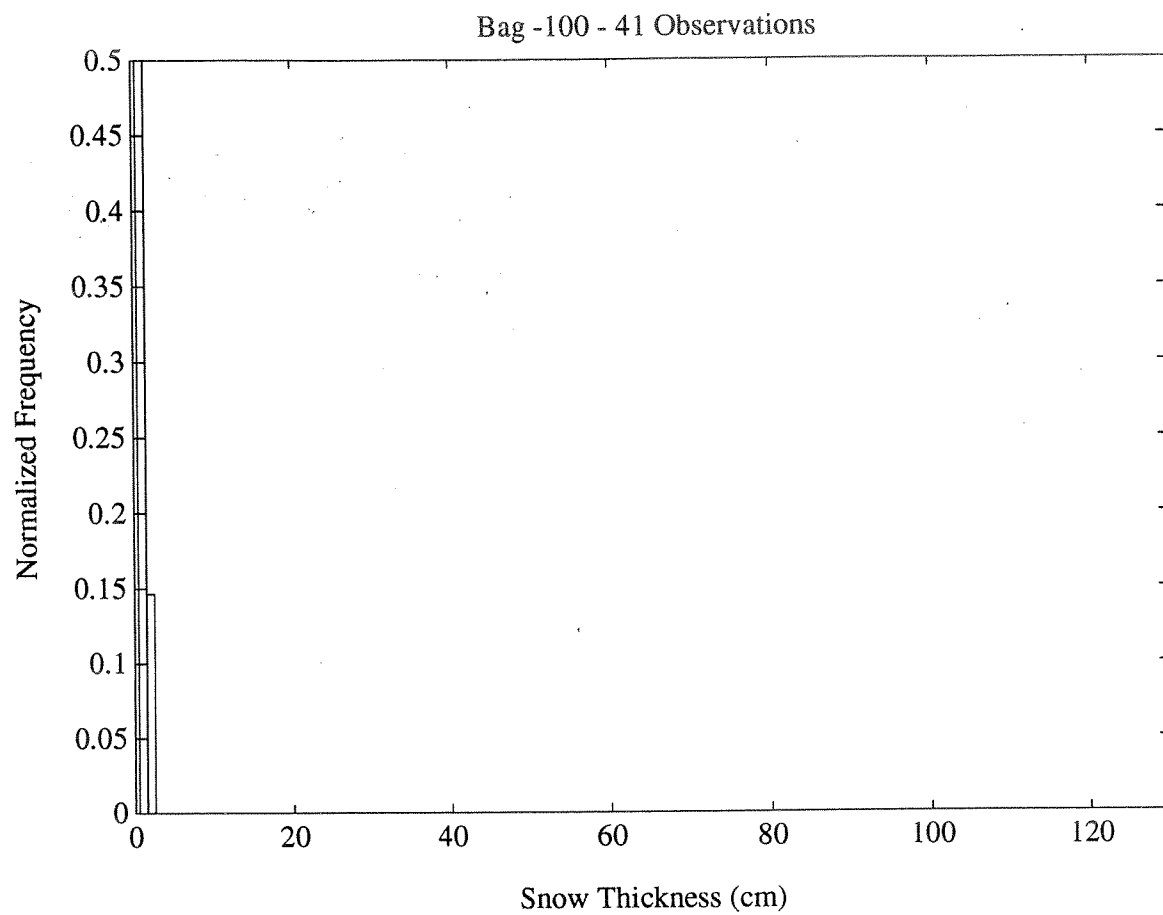


Bag -300 - 41 Observations

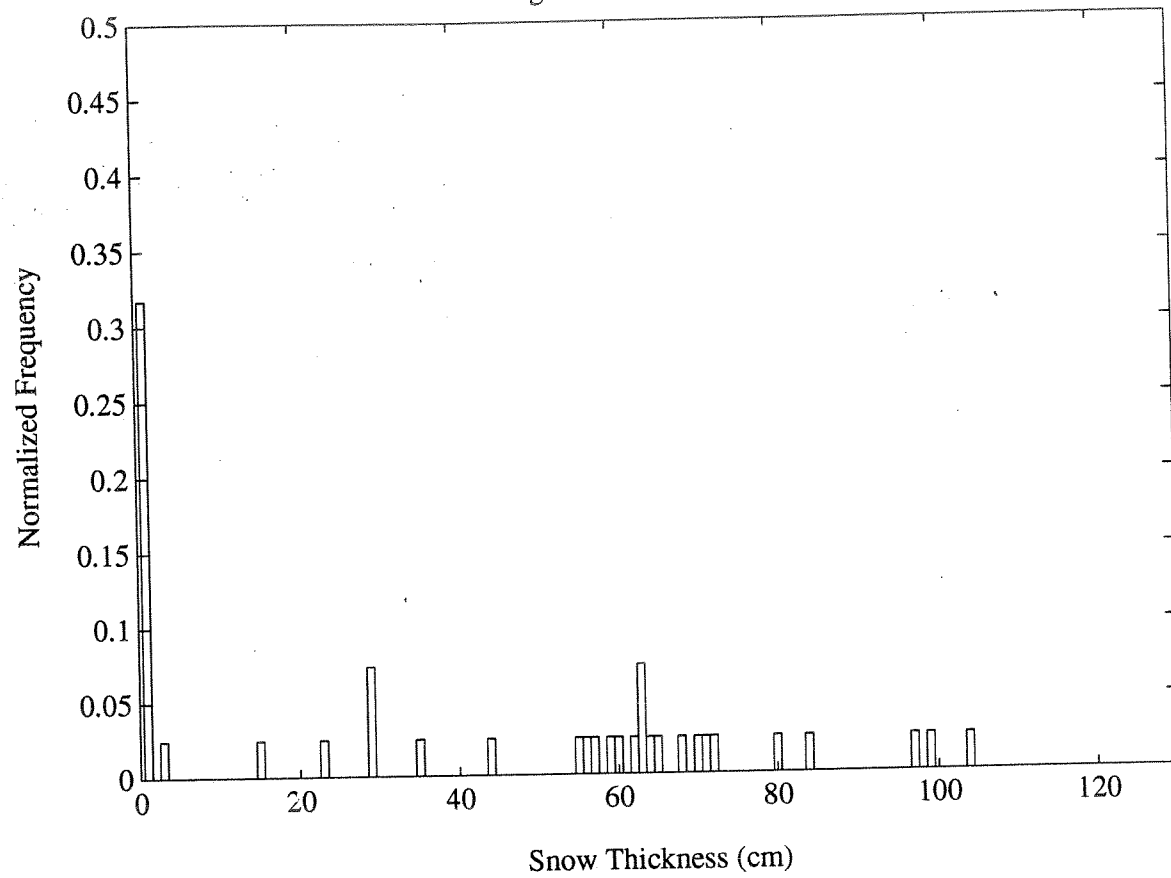


Bag -200 - 41 Observations

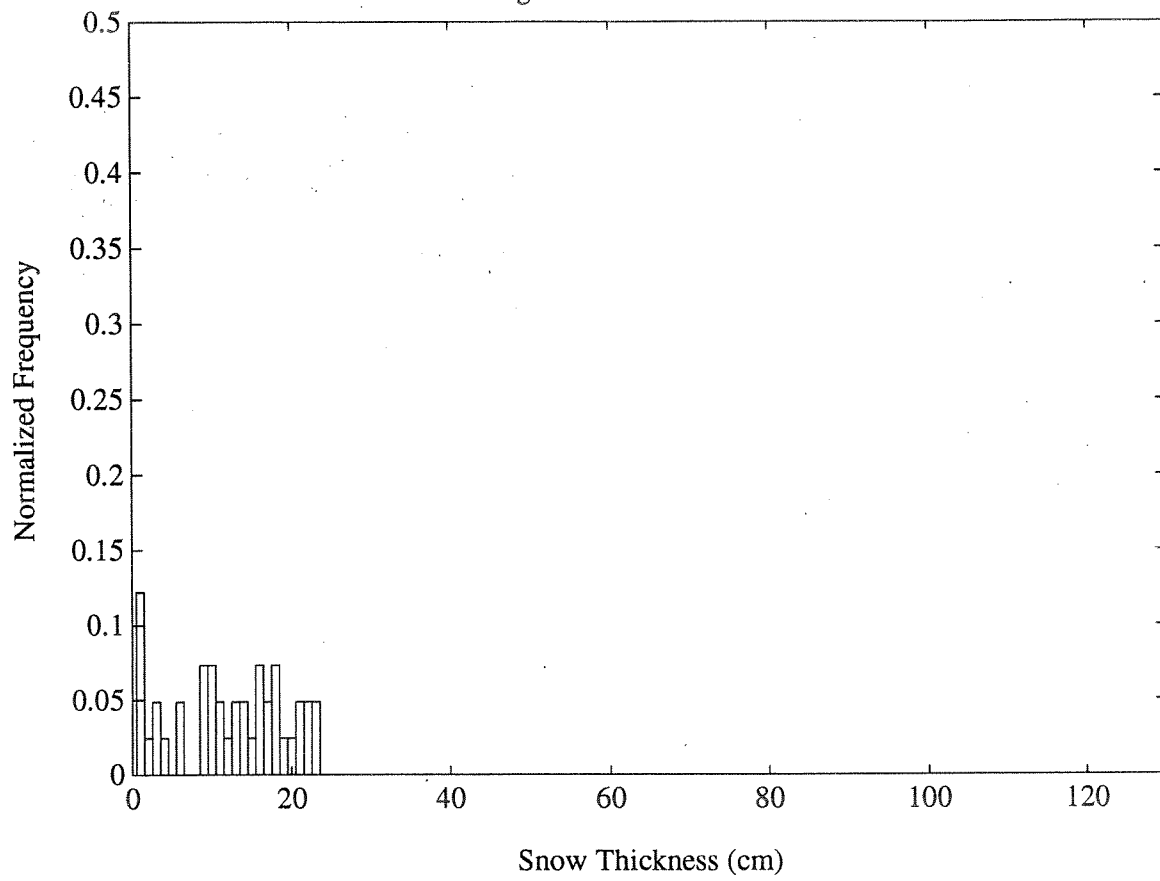




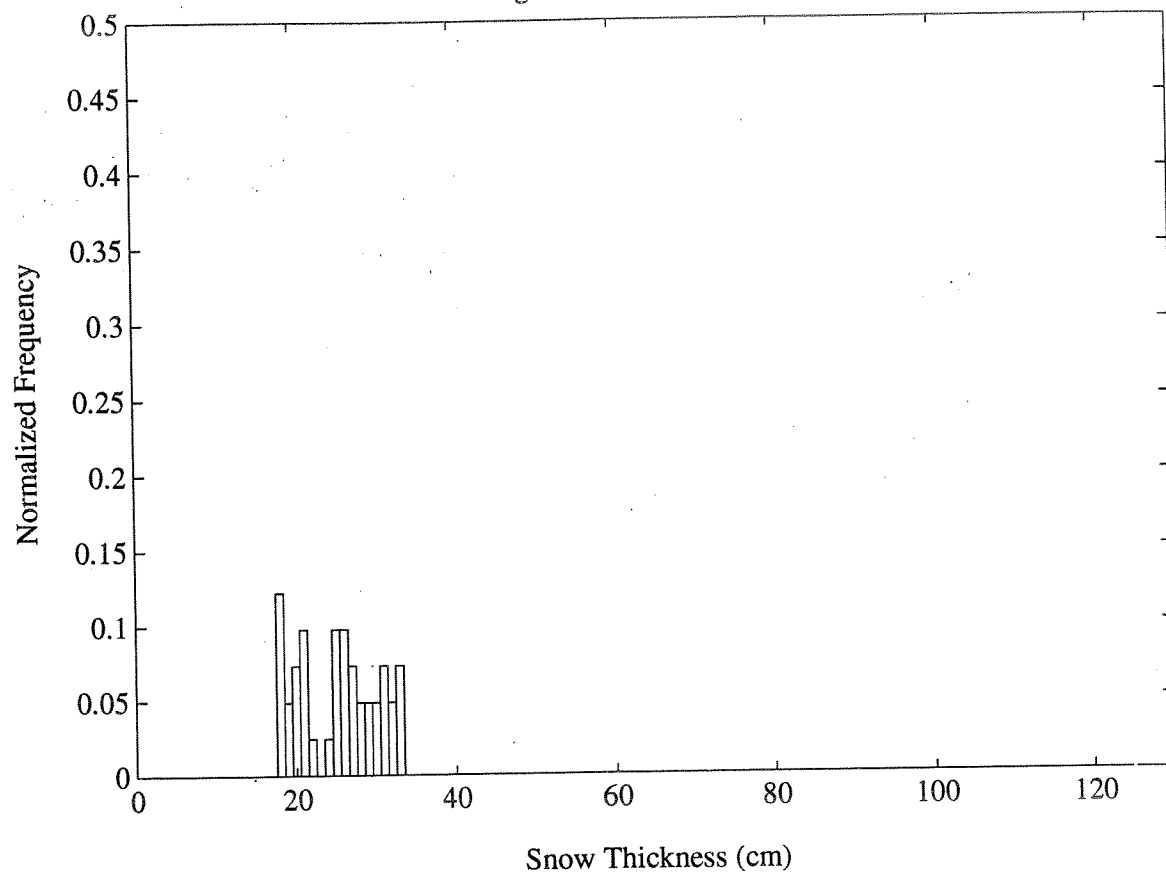
Bag 0 - 41 Observations



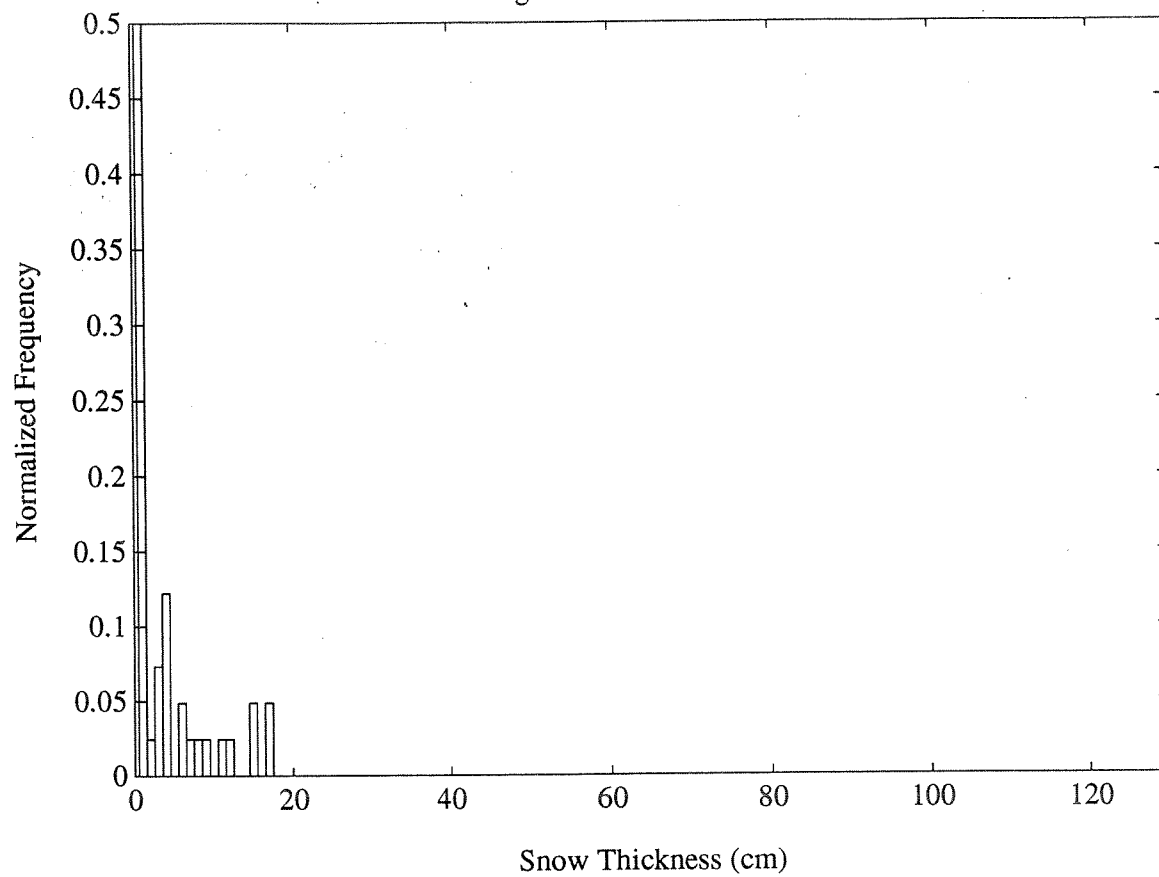
Bag 100 - 41 Observations



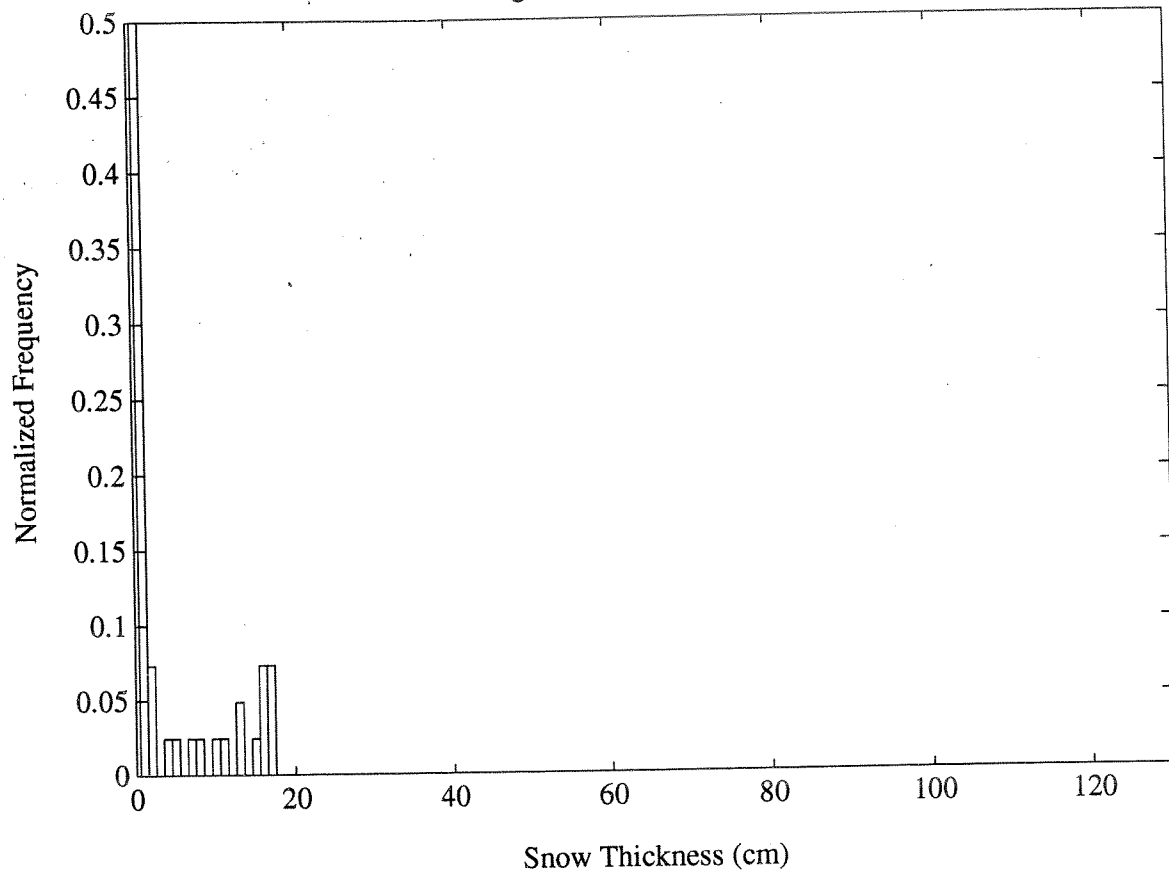
Bag 200 - 41 Observations



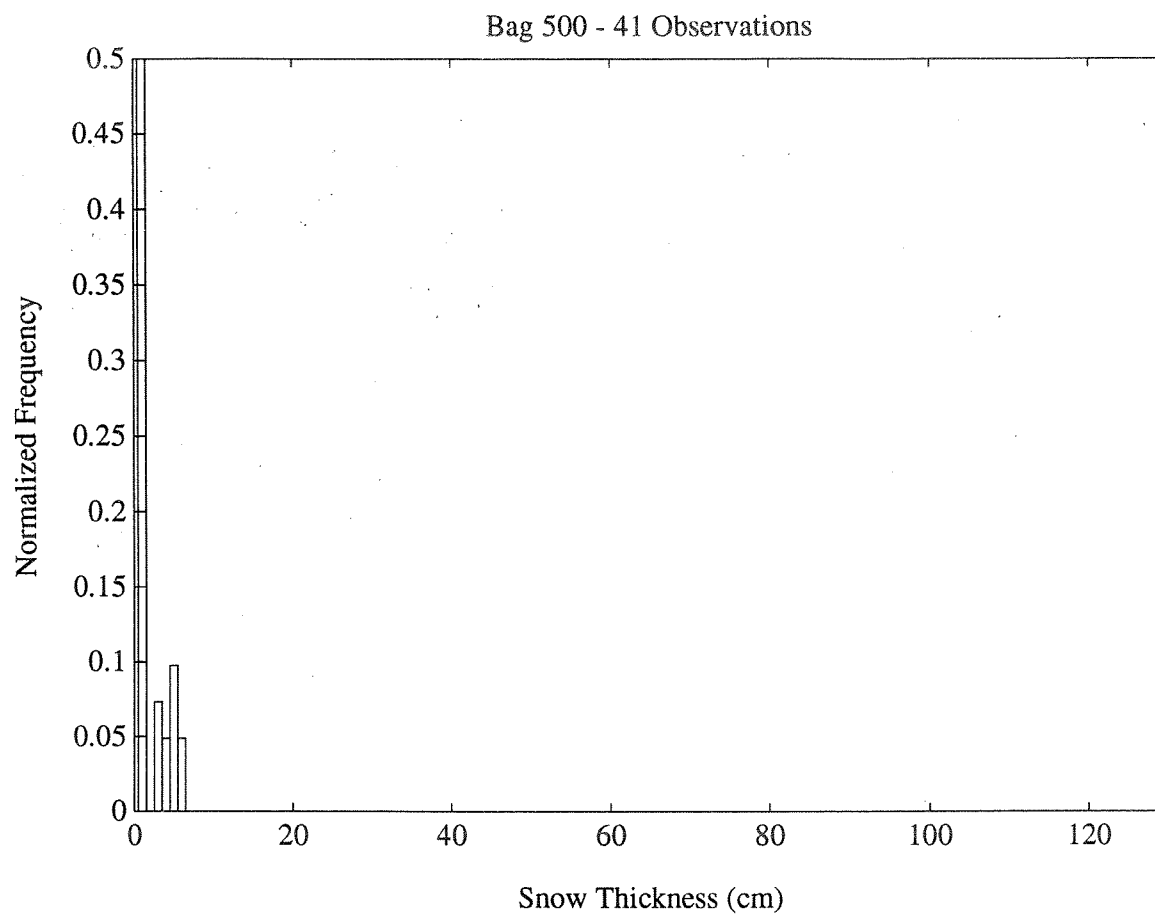
Bag 300 - 41 Observations



Bag 400 - 41 Observations

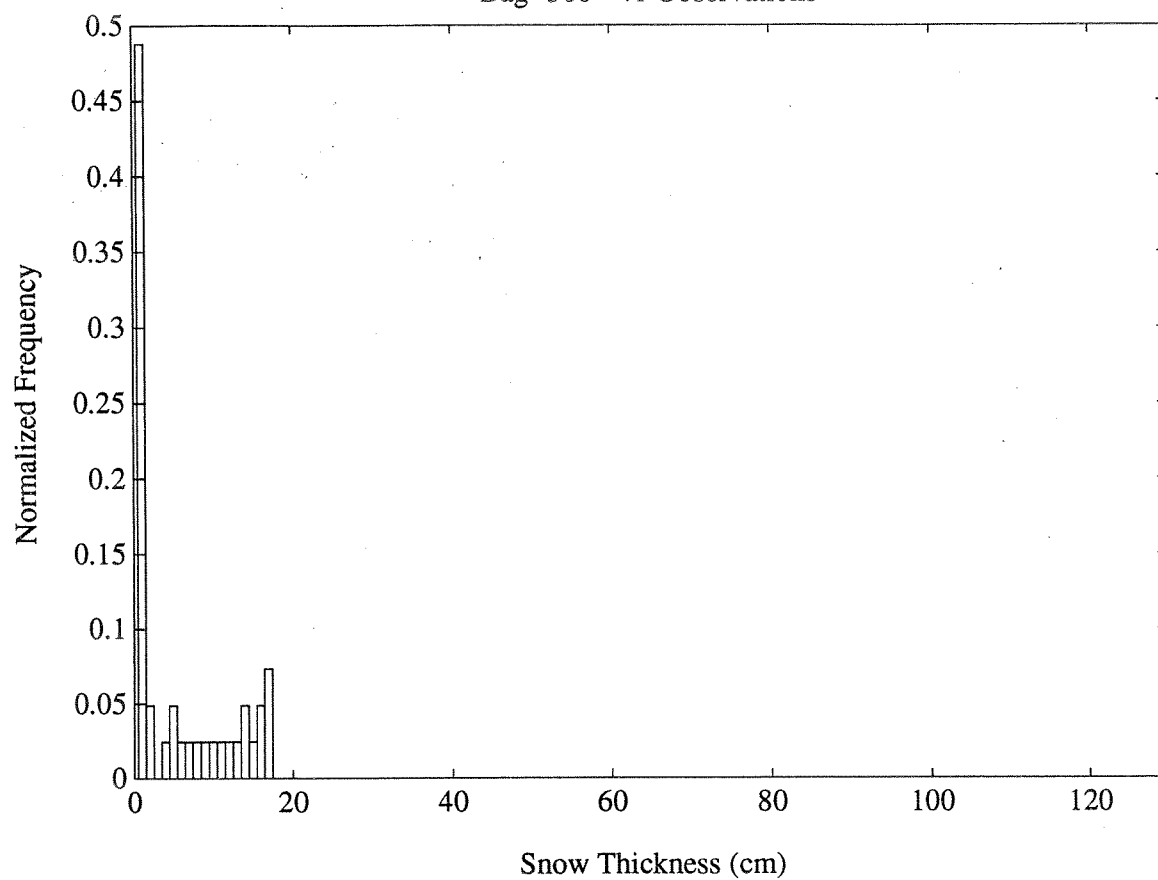


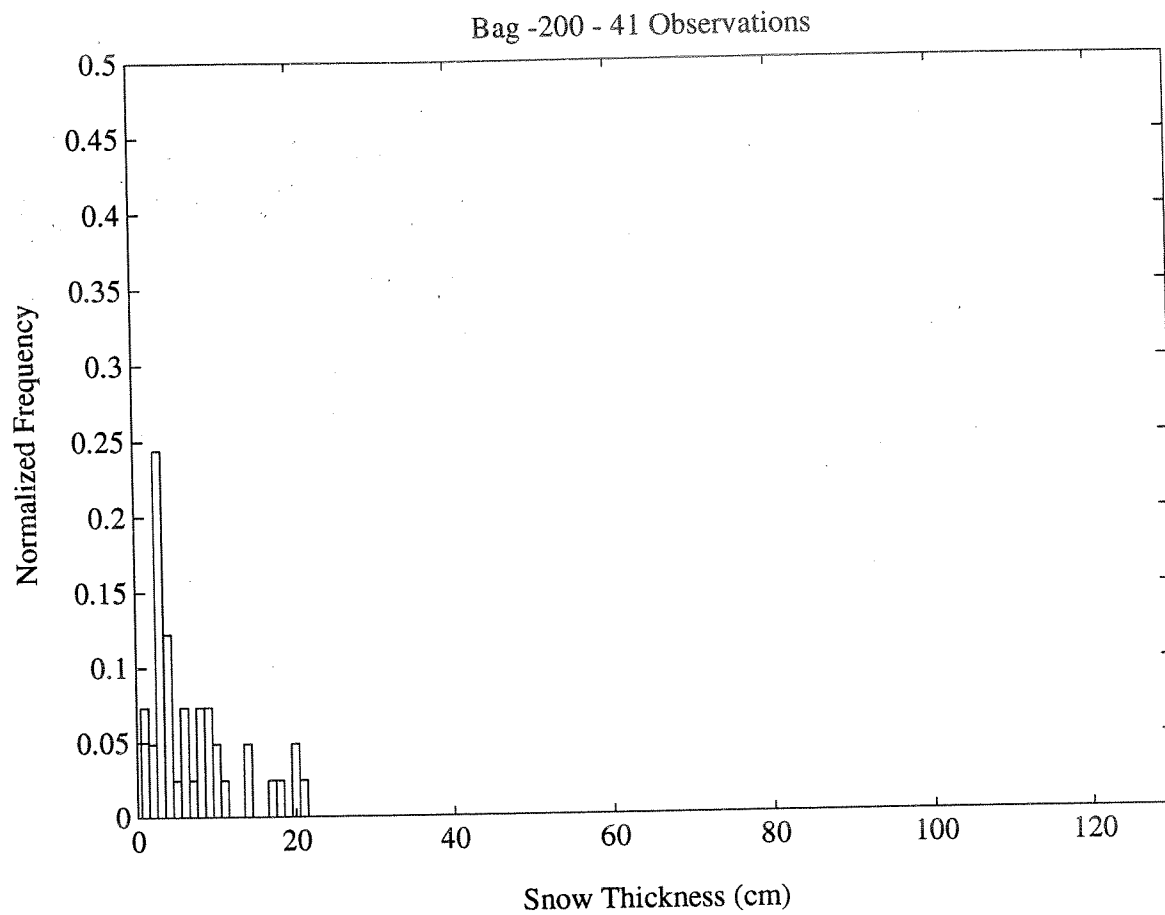




**Histograms for line SHEAR3.**

Bag -300 - 41 Observations





Bag -100 - 41 Observations

